Article

SOURCE DATA | TRANSPARENT PROCESS

THE EMBO JOURNAL

Eaf5/7/3 form a functionally independent NuA4 submodule linked to RNA polymerase II-coupled nucleosome recycling

Dorine Rossetto[1], Myriam Cramet[1,‡], Alice Y Wang[2,‡,§], Anne-Lise Steunou[1,‡], Nicolas Lacoste[1,†], Julia M Schulze[2,¶], Valérie Côté[1], Julie Monnet-Saksouk[1], Sandra Piquet[1], Amine Nourani[1], Michael S Kobor[2] & Jacques Côté[1,*]

Abstract

The NuA4 histone acetyltransferase complex is required for gene regulation, cell cycle progression, and DNA repair. Dissection of the 13-subunit complex reveals that the Eaf7 subunit bridges Eaf5 with Eaf3, a H3K36me3-binding chromodomain protein, and this Eaf5/7/3 trimer is anchored to NuA4 through Eaf5. This trimeric subcomplex represents a functional module, and a large portion exists in a native form outside the NuA4 complex. Gene-specific and genome-wide location analyses indicate that Eaf5/7/3 correlates with transcription activity and is enriched over the coding region. In agreement with a role in transcription elongation, the Eaf5/7/3 trimer interacts with phosphorylated RNA polymerase II and helps its progression. Loss of Eaf5/7/3 partially suppresses intragenic cryptic transcription arising in *set2* mutants, supporting a role in nucleosome destabilization. On the other hand, loss of the trimer leads to an increase of replication-independent histone exchange over the coding region of transcribed genes. Taken together, these results lead to a model where Eaf5/7/3 associates with elongating polymerase to promote the disruption of nucleosomes in its path, but also their refolding in its wake.

Keywords histone acetylation; NuA4; nucleosome dynamics; transcription elongation

Subject Categories Chromatin, Epigenetics, Genomics & Functional Genomics; Transcription

DOI 10.15252/embj.201386433 | Received 29 July 2013 | Revised 14 April 2014 | Accepted 17 April 2014 | Published online 19 May 2014

The EMBO Journal (2014) 33: 1397–1415

Introduction

Specific post-translational modifications of histones within chromatin play critical roles in nuclear functions. Evolutionarily conserved acetylation of histone N-terminal domains was the first covalent modification to be shown to be a key regulator of a nuclear process, that is, transcription. Multiple other histone modifications such as phosphorylation, methylation, and ubiquitination have also since emerged as important players in transcription regulation, defining the chromatin state (Bannister & Kouzarides, 2011; Zentner & Henikoff, 2013). Methylation of histone H3 on lysines 4, 36, and 79 has been linked to the elongation of transcription (Shilatifard, 2006). While some modifications have the potential of directly modulating chromatin structure, they can also be recognized as specific marks by protein modules within regulators (Yun *et al*, 2011; Musselman *et al*, 2012). Classical examples of these protein module–histone mark interactions are the bromodomains with specific acetylated lysines and chromodomains (CHDs) with methylated lysines. These interactions are believed to play an important role for retention/accumulation of specific regulatory factors at chromosomal loci. Furthermore, cross talk between different histone modifications has been demonstrated (Suganuma & Workman, 2011).

Nucleosome acetyltransferase of H4 (NuA4) is a large multisubunit complex that acetylates histone H2A, H2A.Z and H4 N-termini in chromatin (Allard *et al*, 1999; Boudreault *et al*, 2003; Babiarz *et al*, 2006; Keogh *et al*, 2006). Its catalytic subunit Esa1 is the only essential histone acetyltransferase (HAT) in yeast (Smith *et al*, 1998; Clarke *et al*, 1999). Initial purifications of the NuA4 complex showed 13 stable subunits including ATM-related factor Tra1 (shared with the SAGA complex), enhancer of polycomb homolog Epl1, actin-related protein Arp4, leukemogenic factor ENL/AF9 homolog Yaf9 and initially 7 Esa1-associated factors, Eaf1-7, two of

1 St-Patrick Research Group in Basic Oncology, Laval University Cancer Research Center, Centre de Recherche du CHU de Québec-Axe Oncologie, Hôtel-Dieu de Québec, Quebec City, QC, Canada
2 Center for Molecular Medicine and Therapeutics, Child and Family Research Institute, Vancouver, BC, Canada
*Corresponding author. Tel: +1 418 525 4444, ext. 15545; E-mail: Jacques.Cote@crhdq.ulaval.ca
‡These authors contributed equally to this work
†Present address: Institut Curie/CNRS, UMR3664, Paris, France
§Present address: Hotchkiss Brain Institute, Faculty of Medicine, University of Calgary, Calgary AB, Canada
¶Present address: Department of Medical and Applied Genetics, University of Tübingen, Tübingen, Germany

which now bear the names Yng2 (Eaf4) and Swc4 (Eaf2) (Doyon & Cote, 2004; Altaf *et al*, 2009). NuA4 has been implicated in the regulation of gene transcription through local recruitment by DNA-bound transcription factors (Utley *et al*, 1998; Reid *et al*, 2000; Rohde & Cardenas, 2003; Nourani *et al*, 2004; Mitchell *et al*, 2008; Joo *et al*, 2011) or by histone marks and other regulators (Morillon *et al*, 2005; Ginsburg *et al*, 2009; Uprety *et al*, 2012). But NuA4 function is not only restricted to transcription as it was also shown to be important for the cellular response to DNA damage and to play a direct role for the repair of DNA double-strand breaks (Bird *et al*, 2002; Choy & Kron, 2002; Boudreault *et al*, 2003; Downs *et al*, 2004; Lin *et al*, 2008). NuA4 is truly multifunctional as it was also proposed to play a role in chromosome segregation and establishment of chromatin boundaries (Le Masson *et al*, 2003; Krogan *et al*, 2004; Marston *et al*, 2004; Zhang *et al*, 2004; Babiarz *et al*, 2006; Zhou *et al*, 2010; Mitchell *et al*, 2011) and to regulate cellular life span and autophagy through acetylation of non-histone substrates (Lin *et al*, 2009; Lu *et al*, 2011; Yi *et al*, 2012).

It is interesting to note that NuA4 subunits contain several protein domains typical of activities interacting with chromatin, for example, PHD finger, SANT, YEATS, actin-related, and CHDs (Doyon & Cote, 2004) . In fact, NuA4 contains 2 of the 3 yeast proteins that harbor CHDs. In particular, the Eaf3 CHD protein has been shown to regulate the global pattern of histone acetylation *in vivo*, keeping coding regions of long genes at low levels of acetylation, while promoter regions contain more acetylated histones (Reid *et al*, 2004). It is also part of the Rpd3S histone deacetylase complex that binds the coding region of genes to stabilize nucleosomes in the wake of the RNA polymerase II (RNAPII) and suppresses intragenic cryptic/spurious transcription (Carrozza *et al*, 2005; Joshi & Struhl, 2005; Keogh *et al*, 2005; Li *et al*, 2007c). This binding involves an interaction between Set2-dependent H3K36 methylation and Eaf3 chromodomain (Li *et al*, 2007b; Sun *et al*, 2008; Xu *et al*, 2008). Rpd3S, like Set2, follows elongating RNAPII through an interaction with its C-terminal domain (Drouin *et al*, 2010; Govind *et al*, 2010). Competition between Eaf3-containing HAT (NuA4) and HDAC (Rpd3S) complexes is thought to occur during transcription (Biswas *et al*, 2008), and NuA4-dependent acetylation of chromatin has been suggested to help chromatin remodeling during transcription elongation (Carey *et al*, 2006; Ginsburg *et al*, 2009).

Recent work has begun to identify functional modules/subcomplexes within the large NuA4 complex, with a central role of Eaf1 as assembling platform (Auger *et al*, 2008; Mitchell *et al*, 2008). For example, picNuA4 is formed of Esa1, Epl1, and Yng2 and has been implicated in global non-targeted acetylation of chromatin (Boudreault *et al*, 2003; Friis *et al*, 2009). Tra1 is an interface for interaction with activators and is shared with the SAGA HAT complex (Brown *et al*, 2001). Arp4 and Act1 are also found in the INO80 chromatin remodeling complex involved in DNA repair, while Swc4, Yaf9, Arp4, and Act1 are also part of the SWR1 complex (SWR1-C), which is responsible for incorporation of the H2AZ histone variant in euchromatin (Shen *et al*, 2000; Krogan *et al*, 2003; Kobor *et al*, 2004; Mizuguchi *et al*, 2004; Zhang *et al*, 2004; Auger *et al*, 2008). We showed that NuA4 is conserved in higher eukaryotes and corresponds to the human Tip60 complex (Doyon *et al*, 2004). While homologs of 12 of the 13 yeast NuA4 subunits are present in the human complex, additional human subunits led us to propose that the Tip60 complex is a physical merge of two yeast complexes, NuA4 and SWR1-C, through a fusion of the Eaf1 and Swr1 proteins into p400 in mammals (Doyon & Cote, 2004; Auger *et al*, 2008; Altaf *et al*, 2009). The two separate yeast activities have been shown to have close functional ties, primarily converging on the biology of histone variant H2A.Z (Kobor *et al*, 2004; Babiarz *et al*, 2006; Keogh *et al*, 2006; Millar *et al*, 2006; Durant & Pugh, 2007; Auger *et al*, 2008; Kim *et al*, 2009; Altaf *et al*, 2010; Zhou *et al*, 2010).

In order to define specific function(s) of subunits in the NuA4 complex, we pursued genetic and biochemical analysis of a group of poorly characterized Esa1-associated factors. Here, we demonstrate that Eaf7 associates with Eaf5 and the CHD-containing protein Eaf3 and that this trimer defines a new functional subcomplex in NuA4. Our data indicate that this trimer also exists independently of NuA4 in the cell and is found on the coding regions of actively transcribed genes. Even though it is functionally linked to the Set2 histone H3K36 methyltransferase, its genome-wide localization appears independent of Eaf3 and physically linked to elongating RNAPII. We demonstrate that loss of the trimer affects Pol II kinetics, can partially suppress intragenic spurious transcription arising in *set2* mutant cells, and leads to increased histone exchange on a transcribed coding region. Altogether, our results identify a new functional trimeric protein complex important for the transcription elongation process that plays a role in nucleosome destabilization and recycling.

Results

Purification of Eaf5, Eaf6, and Eaf7 shows that they are stable subunits of the NuA4 HAT complex

When we first affinity purified the yeast NuA4 HAT complex to homogeneity, we identified 6 uncharacterized yeast proteins, named Esa1-associated factors 1–6 (Eaf1-6) (Galarneau *et al*, 2000; Eisen *et al*, 2001; Nourani *et al*, 2001). Neither Eaf5 nor Eaf6 had known domains or obvious phenotypes. No clear homolog of Eaf5 is found in higher eukaryotes, while Eaf6 has a homologous protein in the human Tip60/NuA4 complex (Doyon & Cote, 2004; Doyon *et al*, 2004), HBO1, and MOZ/MORF HAT complexes (Doyon *et al*, 2006). Later on, using the tandem affinity purification (TAP) approach, we purified a large amount of NuA4 complex using the subunit Epl1 (Boudreault *et al*, 2003; Auger *et al*, 2008; see Fig 1A, lane 1), and a thirteenth subunit, Eaf7, was identified based on high peptide coverage obtained by mass spectrometry, similar to the other subunits (48 peptides, 62% of protein length). This protein, which shows no special features aside from being highly charged, was also identified in NuA4 purifications by other groups (Krogan *et al*, 2004; Mitchell *et al*, 2008). Eaf7 was likely initially missed because its highly charged nature (pI 5.0; predicted molecular weight 49 kDa) generates a smeary band that varies from one gel to another and stains poorly (Fig 1A and Supplementary Fig S1B, C and D). The use of Eaf5 instead of Epl1 as a bait in TAP purification not only confirms the stable association of Eaf5 itself with the NuA4 complex but also the protein band corresponding to Eaf7 (Fig 1A, lane 2). Interestingly, Eaf5, Eaf7, and the chromodomain protein Eaf3 are recovered at higher levels than the other NuA4 subunits (compare lane 1 and 2). This is not the case when Eaf6 is TAP-tagged, which allows the purification of the usual set and intensities of NuA4 components

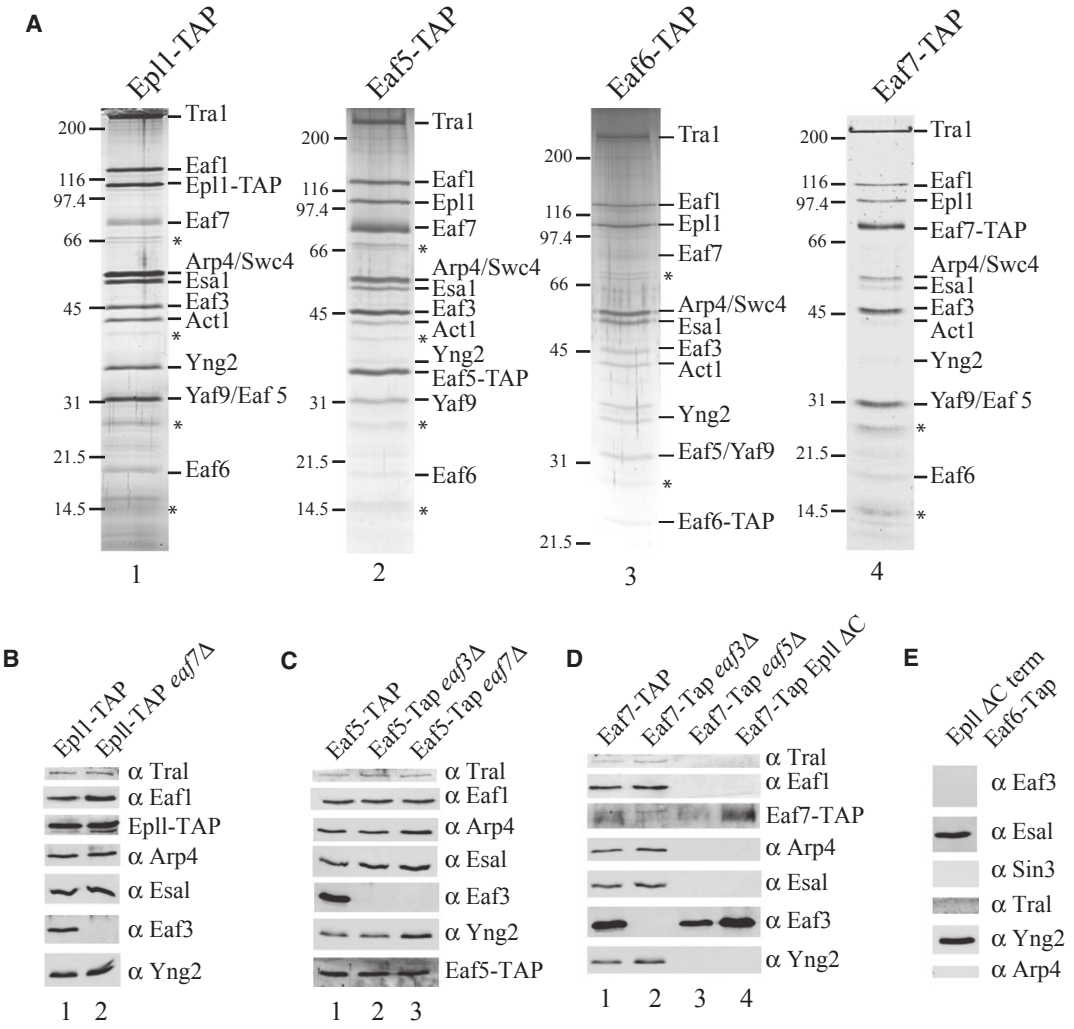

Figure 1. Eaf5, Eaf6, and Eaf7 are stable subunits of the NuA4 HAT complex, and Eaf5 anchors Eaf7 and chromodomain-containing Eaf3 to the rest of NuA4.

A Yeast strains expressing Epl1, Eaf5, Eaf7, or Eaf6 with the TAP (tandem affinity purification) cassette at their C termini were produced by homologous recombination. Affinity-purified complexes from 6 L cultures were run on SDS-PAGE and silver-stained. Known NuA4 components are labeled on the right based on molecular weight and mass spectrometry. *marks non-specific bands.

B Purification of NuA4 from an *EAF7*-deleted strain shows the specific loss of the Eaf3 subunit. Epl1-TAP-purified complexes from 250 ml cultures of wild-type and *eaf7*Δ strains were run on a 10% SDS-PAGE, transferred onto nitrocellulose membrane and detected with the indicated antibodies.

C Eaf7 is required for Eaf3 association to NuA4, but Eaf5 is not affected. *EAF3* or *EAF7* genes were deleted in an Eaf5-TAP-expressing strain. Purified complexes from 250 ml cultures were analyzed as in (B).

D Eaf5 anchors Eaf7 and Eaf3 to the NuA4 complex**.** *EAF3* or *EAF5* genes were deleted in an Eaf7-TAP-expressing strain. Eaf7-TAP was also produced in an Epl1(1-485)-expressing strain (Epl1ΔC, in which Esa1/Epl1/Yng2 (picNuA4) is separated from the rest of NuA4; Boudreault *et al*, 2003). Affinity-purified complexes were analyzed as in (B). Note that Tra1 and Eaf1 are not detected by Western blot in lanes 3 and 4 but corresponding faint bands are seen in lane 4 on the silver-stained gel (Supplementary Fig S1D).

E Eaf6 is associated with picNuA4, the catalytic subcomplex of NuA4. Eaf6-TAP was produced in an Epl1(1-485)-expressing strain (ΔC Term) and analyzed by Western blot.

Source data are available online for this figure.

(lane 3). The stable association of Eaf7 with NuA4 was confirmed by directly tagging and purifying the protein (Fig 1A, lane 4). Eaf7 is clearly a stable subunit of NuA4 as it copurifies with the same set of polypeptides (note that the relative intensities are similar to the ones obtained with Eaf5-TAP). Histone acetyltransferase activity of the Eaf7-purified complex was also analyzed and is again identical to NuA4 complexes purified through other tags or methods (Supplementary Fig S1A).

Eaf5 anchors Eaf7/Eaf3 to the rest of the NuA4 complex

In order to understand the role of Eaf7 in the structure of NuA4, we purified the complex from cells lacking the *EAF7* gene. The Western blot analysis (Fig 1B) and the silver-stained gel (Supplementary Fig S1B) clearly show that the loss of Eaf7 subunit in NuA4 does not disrupt its assembly since 11 of the original subunits are still present. On the other hand, the data indicate that association of the Eaf3

chromodomain subunit is completely lost in the absence of Eaf7. We also used the Eaf5-TAP-expressing strain for NuA4 purification and found similar results as with the Epl1-TAP strain (Fig 1C and Supplementary Fig S1C). In *eaf7*Δ cells, NuA4 loses subunits Eaf3 and Eaf7, while purification of Eaf5-TAP from an *eaf3*Δ strain shows apparently only loss of Eaf3 (lane 2). No definitive answer is obtained for Eaf7 in the latter case though the smeary signal on gel appears unaffected (Supplementary Fig S1C, lane 2). To pursue Eaf7 interacting partners within NuA4, we used Eaf7-TAP-expressing cells (Fig 1D and Supplementary Fig S1D). While Eaf7-TAP purification yields the full native NuA4 complex, deletion of *EAF3* does not disrupt this purification as all NuA4 subunits are recovered, except Eaf3 (lane 2). This indicates that Eaf3 is not required for Eaf7 association to NuA4, while conversely Eaf7 is necessary for Eaf3 (Fig 1B, lane 2). Interestingly, when *EAF5* is deleted, all NuA4 subunits are lost in the Eaf7-TAP purification, except Eaf3 (Fig 1D, lane 3). This indicates that Eaf7 is not associated with NuA4 in the absence of Eaf5 but is still bound to Eaf3. Finally, we purified Eaf7 from a strain that contains a truncated version of NuA4 subunit Epl1. In these cells, the catalytic HAT subcomplex of NuA4, picNuA4, is separated from the rest of the complex, allowing only global non-targeted acetylation of H4/H2A in chromatin (Boudreault *et al*, 2003). Eaf7-TAP purification clearly shows that Eaf7 is still associated with Eaf3 and Eaf5 but not with picNuA4 components (Esa1, Epl1, Yng2) (Fig 1D, lane 4 and Supplementary Fig S1D), which is in clear contrast to purification of Eaf6 in the same background (Fig 1E and Supplementary Fig S1G). Western blot analysis suggests that Eaf3/5/7 are not associated with the rest of NuA4 either, but closer analysis of the silver-stained gel shows weak specific bands for Eaf1 and Tra1 subunits (Supplementary Fig S1D). This concurs with our previous results in which we showed that Eaf1 was the platform for NuA4 assembly and that purification of Eaf5-TAP from an *eaf1*Δ strain yielded only Eaf5/7/3 (Auger *et al*, 2008). Altogether, our results indicate that Eaf7 forms a bridge between Eaf5 and Eaf3 proteins and Eaf5 anchors the trimer to Eaf1 and the rest of NuA4. In contrast, Eaf6 resides within the piccolo NuA4 subcomplex, consistent with recent results we obtained with the homologous human protein (Avvakumov *et al*, 2012).

Interestingly, Eaf3 chromodomain protein, but not Eaf5/Eaf7, is also part of the Rpd3S histone deacetylase complex (Carrozza *et al*, 2005; Keogh *et al*, 2005). Using Eaf3-TAP-expressing cells in parallel with Epl1-TAP and Sin3-TAP, we found that a much larger portion of cellular Eaf3 seems associated with the HDAC complex (Supplementary Fig S1E and F, compare lanes 1, 4 and 5). As expected, deletion of *EAF5* or *EAF7* has no effect on Eaf3 association with Rpd3S (lanes 2 and 3). The presence of Eaf3 in both HAT and HDAC complexes suggests that its chromodomain plays a similar role in the interaction/spreading of each complex on the chromatin fiber through an interaction with Set2-dependent H3K36me.

Eaf3/5/7 form an independent native complex in yeast cells

Upon closer examination of NuA4 purifications using Eaf3, Eaf5, and Eaf7-TAP strains in comparison with other tagged subunits, we noticed that each protein of the trimer increased the recovery of the two others (e.g., see Fig 1A). While this could be due to their direct physical association, we suspected that this could also reflect their presence in an additional protein complex outside NuA4. To test this hypothesis, we purified Eaf7 and Eaf5 by tandem affinity as before and loaded the purified material on a gel filtration column (Fig 2A and B). Western blot analysis and silver-stained gel of the fractions clearly demonstrate that, while the NuA4 complex elutes as the usual 1.3 MDa complex, the majority of Eaf3, Eaf5, and Eaf7 proteins coelute as a small protein complex (~300–400 KDa). A smaller portion of Eaf5/7/3 also coelutes with the large NuA4 complex. Depending on their three-dimensional conformation, the lower molecular weight fractions could contain uniquely the trimeric complex with no other stably associated proteins, as indicated by mass spectrometry analysis (data not shown). The existence of a native separate Eaf5/7/3 trimer in the cell indicates that these three proteins do represent a functional entity that works within NuA4 but also by itself. Based on our results and previous work, a schematic representation of the different functional modules/subcomplexes of NuA4 is presented in Fig 2C.

Eaf3, eaf5, and eaf7 mutant cells share similar phenotypes

In order to get clues about Eaf3/5/6/7 roles in NuA4 function, we tested deletion mutant strains on different media (Fig 3 and Supplementary Fig S2). All mutant strains have no defects in normal growth conditions in rich media. On the other hand, *eaf3, eaf5,* and *eaf7* cells are sensitive to temperature, while *eaf6* cells are not (Fig 3A). Growth defects in the presence of DNA-damage-inducing drugs like methyl methanesulfonate (MMS) are a typical phenotype of NuA4 mutants (Boudreault *et al*, 2003; Downs *et al*, 2004; Auger *et al*, 2008), but none of the cells tested here show sensitivity. In contrast, *eaf3/5/7* mutant cells are incapable of growth in presence of rapamycin, an inhibitor of the Tor kinase pathway and another typical phenotype of NuA4 mutants, presumably because of its role in ribosomal protein gene expression (Reid *et al*, 2000; Doyon & Cote, 2004; Auger *et al*, 2008). Other potential phenotypes analyzed include growth on glycerol, at 16 degrees, in the presence of formamide, caffeine, 6-azauracil, MPA, or hydroxyurea and defect in telomeric silencing. Significant growth defects are detected for *eaf5/7* mutant cells on 3% formamide, but no other media (Fig 3B and data not shown). Phenotypic analysis of *eaf3* mutant cells is complicated by the presence of the protein in both NuA4 and Rpd3S, two activities with clearly opposing functions (Biswas *et al*, 2008). Nevertheless, almost identical phenotypes between *eaf5* and *eaf7* mutant cells and some similar ones with *eaf3* mutants support our findings of these three proteins contacting each other within NuA4 and suggest that the trimer forms a functional subcomplex.

A strong functional interaction is established between NuA4 and SWR1-C, responsible for incorporation of Htz1 (H2A.Z) in chromatin (reviewed in Altaf *et al*, 2009; Altaf *et al*, 2010). Thus, not surprisingly, *eaf5* and *eaf7* mutant cells show synthetic lethality when combined with *swr1* mutation (Supplementary Fig S2A). On the other hand, some phenotypes and genetic interactions support an independent role of the Eaf5/7/3 trimer, outside of NuA4, in agreement with the fractionation study. Large-scale genetic analysis indicates that *eaf5* and *eaf7* mutants show synthetic negative interactions with several other mutants from the NuA4 complex, including *eaf1*, *esa1*, *epl1*, *arp4*, *yng2*, *yaf9,* and *swc4*, suggesting a distinct but related function (Lin *et al*, 2008). Accordingly, growth sensitivity to formamide appears characteristic of the Eaf3/5/7 trimer since a commonly used *esa1* mutant does not show such a phenotype (Fig 3C).

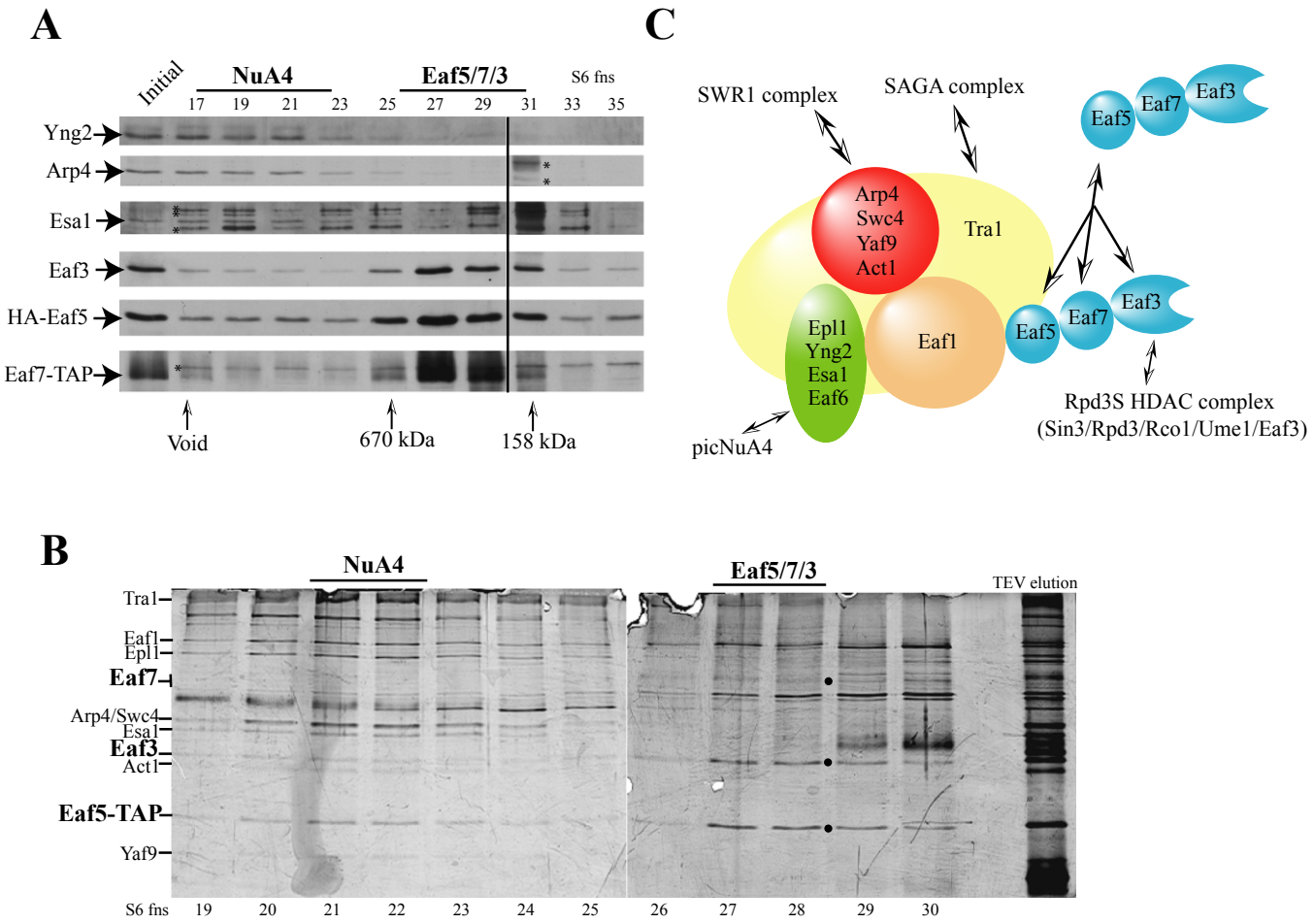

Figure 2. Eaf5, Eaf7, and Eaf3 form a native complex in yeast cells, independent of NuA4.

A Eaf3, Eaf5, and Eaf7 are part of a native complex outside of NuA4. Whole-cell extract from an Eaf7-TAP/HA-Eaf5-expressing strain was submitted to TAP purification. 300 µl of the purified complex was loaded on a superose 6 gel filtration column. Each fraction was then TCA precipitated, resuspended in loading buffer, run on a 10% SDS-PAGE, transferred onto a nitrocellulose membrane, and screened with the indicated antibodies. In the Esa1 lane, asterisks indicate non-specific bands carried over from a previous incubation of the membrane with the anti-TAP antibody (see source data). The vertical bar separates fractions that were run in parallel on different gels.

B A similar experiment was performed using Eaf5-TAP as bait in the purification, and directly loading the TEV elution on the gel filtration column, followed by SDS-PAGE and silver stain. Bands identified by Western blot and mass spectrometry analyses are indicated. Black dots mark the bands corresponding to the Eaf5/7/3 subunits.

C Schematic representation of the different modules associated with NuA4 based on our findings and published work.

Source data are available online for this figure.

Eaf5 and Eaf7 show functional interactions with the Set2 histone methyltransferase

The function of the Eaf5/7/3 trimer is likely related in part to the presence of Eaf3 chromodomain and its interaction with H3K36me2/3 (Eisen *et al*, 2001; Li *et al*, 2007b; Sun *et al*, 2008; Xu *et al*, 2008), a histone mark deposited by the Set2 methyltransferase during the transcription elongation process (reviewed in Li *et al*, 2007a). On the other hand, *set2* mutant cells do not show strong sensitivity to formamide, in contrast to *eaf5/7* cells and cells lacking the H3K4 methyltransferase Set1, a critical player in the early steps of transcription (Fig 3C). Analysis of *set2-eaf5/7* double-mutant cells indicates an aggravated sensitivity to caffeine, suggesting functional interaction during gene expression (Fig 3D). A possible role of the trimer could therefore be during transcription elongation, where Set2 associates with RNAPII and methylates H3K36 in its wake (Li *et al*, 2007a). Sensitivities to nucleotide depletion drugs mycophenolic acid (MPA) and 6-azauracil (6-AU) are frequently used as hallmark of transcription elongation deficiency in yeast cells (Reines, 2003). While our *eaf5/7* and *set2* mutants show no sensitivity on their own, growth defects become evident in the double mutants, most clearly with MPA (Fig 3E and Supplementary Fig S2B). Taken together, these results suggest that the Eaf5/7/3 trimer is functionally linked to histone H3 methylation during transcription elongation but also plays specific distinct roles, partly independent of NuA4 acetyltransferase activity.

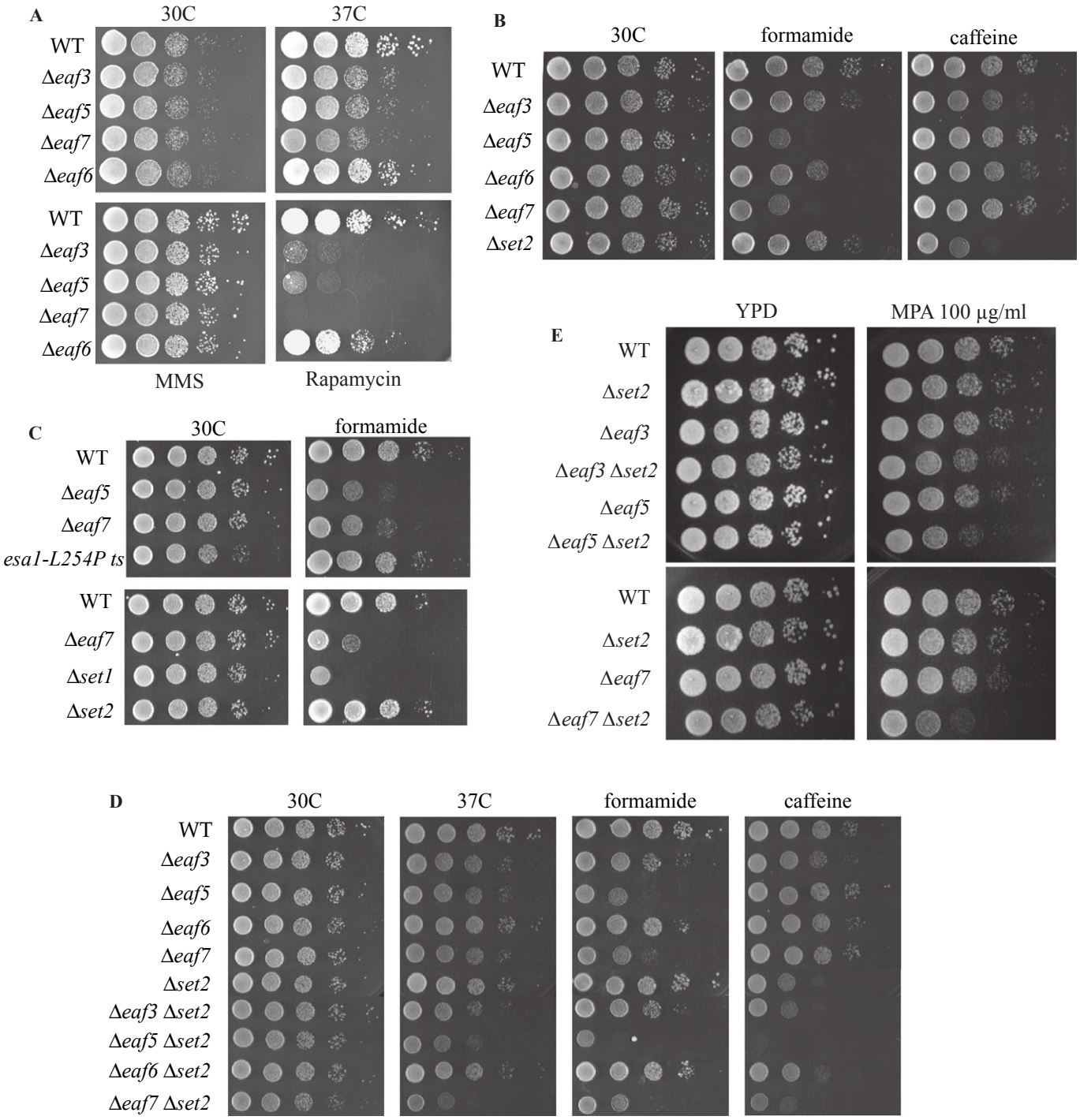

Figure 3. *eaf3*, *eaf5*, and *eaf7* mutant cells show similar phenotypes between them, while distinct from NuA4, and functionally interact with Set2 H3K36 methyltransferase.

A Phenotypic analysis of *eaf3*Δ, *eaf5*Δ, *eaf6*Δ, and *eaf7*Δ cells. Unlike other NuA4 mutants, they are not sensitive to the DNA-damaging agent MMS, but *eaf3*, *eaf5*, and *eaf7* are highly sensitive to rapamycin and significantly sensitive to temperature. 10-fold serial dilutions of indicated strains were spotted on YPD, YPD + MMS (0.015%), or YPD + rapamycin (25 nM) plates and incubated at 30°C or 37°C for 2 days (YPD) or 4 days (MMS and rapamycin).

B *eaf5*Δ and *eaf7*Δ strains are sensitive to formamide. Similar tests as in (A) using formamide and caffeine-containing media.

C Sensitivity to formamide is shared by a *set1* mutant strain but not by *esa1* and *set2* mutants.

D *eaf5*/*set2* and *eaf7*/*set2* double mutants have increased sensitivities to both formamide and caffeine.

E *eaf5*/*set2* and *eaf7*/*set2* double mutants are sensitive to mycophenolic acid, a hallmark of defect in transcription elongation.

The Eaf5/7/3 trimer is enriched over the coding region of specific genes

Since NuA4-dependent acetylation of chromatin has been proposed to facilitate transcription elongation *in vitro* (Carey *et al*, 2006) and *in vivo* by association to coding regions (Ginsburg *et al*, 2009), it was important to determine where Eaf5/7/3 is localized during transcription of a gene. NuA4/Esa1 had already been shown to be enriched on the promoter of active genes (Robert *et al*, 2004; Venters *et al*, 2011), so Epl1-myc was used in parallel to Eaf5/7-myc in ChIP-qPCR experiments on the actively transcribed *PMA1* gene (Fig 4A). When the signals are normalized to the promoter/UAS region of the gene, it becomes apparent that Eaf7 and Eaf5 are preferentially located on the body of the gene, unlike Epl1. These results support a partial physical disconnection of the trimer from the rest of NuA4, as our biochemical fractionations indicated (Fig 2). Eaf7 binding on the *PMA1* coding region is affected by both *EAF5* and *EAF3* deletions but still clearly detected (Fig 4B). Similar results were obtained on the *PGK1* gene (Fig 4C). Since Eaf7 association is still detected in *eaf5* and *eaf3* mutants, this indicates that neither H3K36me nor the NuA4 complex is essential for Eaf7 to bind the coding region of these genes. We next determined whether transcription is essential for this binding using the inducible *GAL1* promoter either in its natural context or fused to the long *FMP27* gene (Mason & Struhl, 2005). As shown in Fig 4D and E, both Epl1-myc and Eaf7-myc signals increase during gene activation and Eaf7 shows the strongest stimulation throughout the coding region. These results demonstrate that Eaf7 binding to coding regions is dependent on ongoing transcription.

NuA4 and the Eaf5/7/3 trimer are globally associated with highly transcribed genes with overlapping but distinct profiles over the transcription units

Previous genome-wide analyses of NuA4 localization have been performed by ChIP-on-chip using microarrays carrying 2–4 probes for each gene (Robert *et al*, 2004; Venters *et al*, 2011). These studies have suggested an enrichment of NuA4 at the promoter of active genes. To obtain very precise profiles of NuA4 and Eaf5/7/3 throughout the yeast genome, we have performed ChIP-on-chip using a RNA-based labeling protocol and very high resolution tiled arrays (overlapping 25 bp probes covering the entire genome), as was used in other recent studies (Schulze *et al*, 2009, 2011). Average signal profiles over open reading frames and intergenic regions were obtained from two independent experiments and are presented in Fig 5 and Supplementary Fig S3. Epl1-myc signals, depicting the NuA4 complex, clearly correlate with the level of gene transcription (Fig 5A and Supplementary Fig S3A). Interestingly, the profile over the transcription unit is different from what has been concluded in previous studies, showing the strongest signal at the promoter/transcription start site but also strong signals throughout the coding region. As a control, anti-Myc ChIP from an untagged strain does not show such strong signals over the coding region (Supplementary Fig S3B). A large portion of the most highly transcribed genes in yeast cells are the ones encoding for ribosomal proteins, which tend to be relatively short. Thus, profiles depicted through the CHROMATRA visualization tool provide a more complete view since it represents signals on all individual genes and throughout their variable lengths (Supplementary Fig S3A) (Hentrich *et al*, 2012). This strong association with ribosomal protein genes certainly accounts for the usual high sensitivity of NuA4 mutant cells to rapamycin, a drug targeting the Tor pathway that regulates ribosome biogenesis (Boudreault *et al*, 2003; Auger *et al*, 2008). Gene-by-gene analysis indicates that most genes bound by Epl1 are also bound by Eaf7, although their distributions along those genes are different (Supplementary Fig S3A; examples in Fig 5E and F, with untagged control in Supplementary Fig S3C and D). Importantly, in comparison, Eaf7-myc signals, while also linked to transcriptional activity, do not show prevalence toward the promoter/transcription start site, but a relatively smooth distribution reaching a maximum over the coding region (Fig. 5B). In other words, while Epl1 and Eaf7 signals over the coding regions are often similar, Epl1 tends to be significantly stronger over the promoter regions. Deletion of *EAF3* does not greatly change Eaf7 profiles, but signals tend to be more evenly distributed between promoter and coding regions, resembling those of Epl1 (Fig 5C; Supplementary Fig S3A). This decrease in Eaf7 preference toward coding regions is likely due to the absence of interaction with H3K36me through Eaf3 over coding regions, consistent with ChIP-qPCR showing that Eaf3 affects but is not essential for Eaf7 binding (Fig 4). Finally, deletion of *EAF5*, which completely disconnects Eaf7–Eaf3 from NuA4 (Fig 1), has a clear effect on the Eaf7-myc signals, specifically affecting gene-specific and average profiles on the promoter but not the coding regions (Fig 5D, E and F; Supplementary Fig S3A). These results indicate that Eaf7 binding to promoter regions is dependent on its association with NuA4, while it is not the case over the coding regions. We conclude that the remaining Eaf7 signals over the body of genes represent native binding sites of the Eaf5/7/3 trimeric complex. Interestingly, when comparing Eaf7 average binding profile over ribosomal protein (RP) genes versus highly transcribed non-RP genes, the preferential association to coding regions is even more pronounced (Supplementary Fig S4A–F).

Deletion of *EAF7* affects RNA polymerase II dynamics during transcription elongation

Based on the preferred binding of Eaf5/7/3 to the coding region of actively transcribed genes, we performed multiple ChIP-qPCR analyses of different histone marks in mutant backgrounds to shed light on the specific function of this small complex. Transcription-linked marks like H3ac, H4ac, H3K4me, and H3K36me do not seem greatly affected in a reproducible manner (data not shown). Of course, histone acetylation/deacetylation during transcription elongation is thought to be very dynamic, and an effect on steady-state levels could be difficult to detect, more so if directly linked to nucleosome stability. Thus, we turned our attention to the RNA polymerase, using the integrated GAL-*FMP27* system to characterize RNAPII progression in different mutant backgrounds. This system utilizes the transcription repression obtained by shifting cells to glucose media in order to characterize the last wave of RNAPII passing through the coding region, by ChIP analysis. This allows determination of *in vivo* transcription elongation rates and polymerase processivity (Mason & Struhl, 2005). Using this system, it has been argued that NuA4 and SAGA HAT complexes cooperate to stimulate transcription elongation rate (Ginsburg *et al*, 2009). Looking at fully activated GAL-*FMP27*, we see that RNAPII steady-state binding over

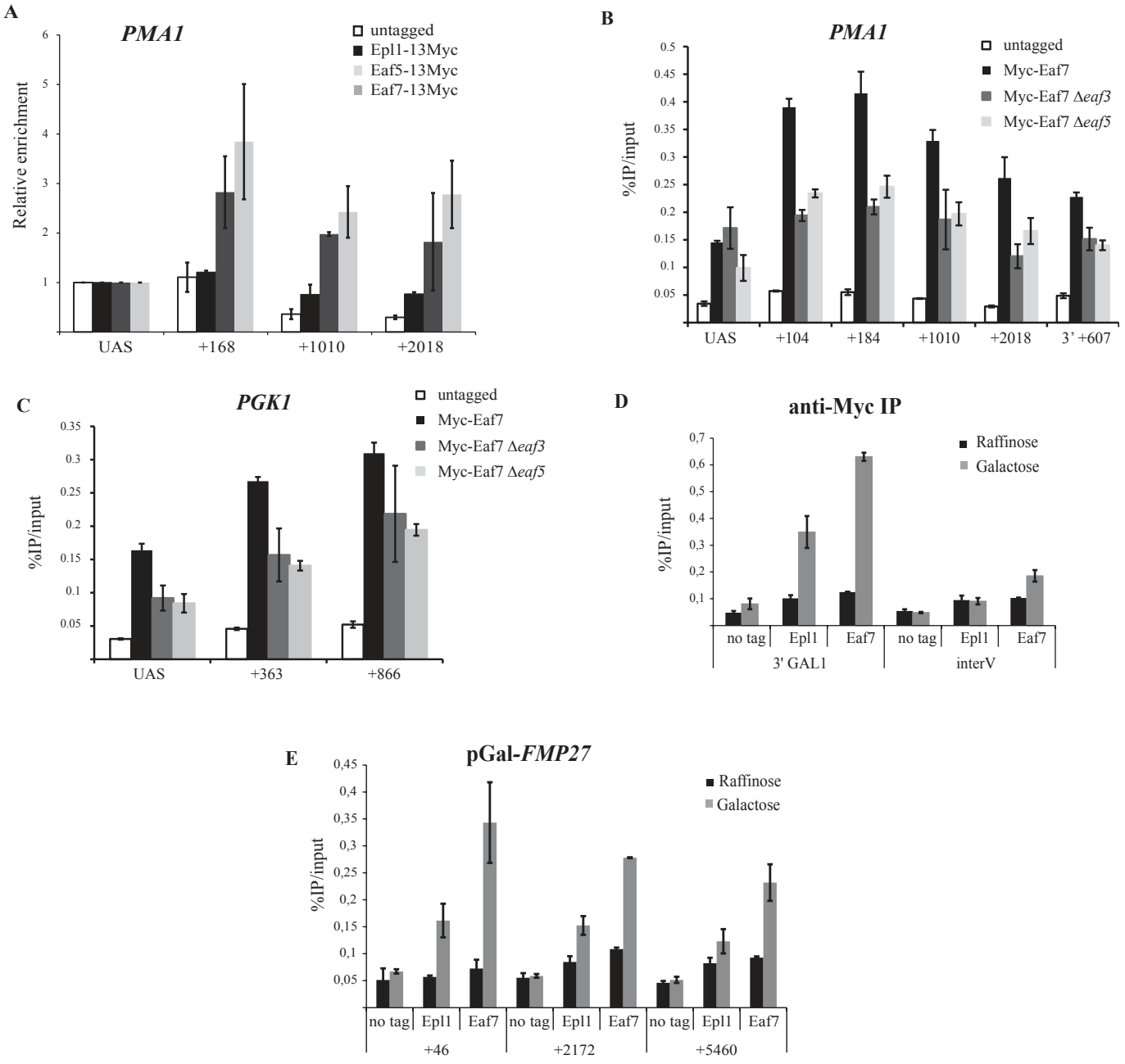

Figure 4. The Eaf5/7/3 trimer is enriched over the coding region of specific genes and is linked to transcriptional activity.

A Anti-Myc ChIP-qPCR on untagged, Epl1, Eaf5, and Eaf7 Myc-tagged strains depicting enrichment of the signals over the coding region of *PMA1*, relative to signals in promoter/UAS set to 1.

B Anti-Myc ChIP-qPCR over the *PMA1* gene of Eaf7-Myc in WT, *eaf5*, *eaf3*, and untagged background.

C Same as (B) but analyzing the binding to the *PGK1* gene.

D, E Anti-Myc ChIP-qPCR of Epl1-myc and Eaf7-myc on *GAL1* (D), pGAL-*FMP27* (E) and control intergenic region, before and after activation by shifting the cells from raffinose to galactose media.

Data information: All ChIP-qPCR data are the average of at least two biological repeats with standard errors.

the coding region is not greatly affected in *set2*, *eaf3*, *eaf5*, and *eaf7* mutant backgrounds (Fig 6A). On the other hand, *set2* and *eaf3* seem to slightly increase pol II signal near the transcription start site (+46), while *eaf7* decreases it. During the time course of repression in glucose media, Pol II is seen disappearing rapidly at the 5′ of the coding region but does so at later time points over downstream regions (Fig 6B). In the *set2* mutant background, Pol II elongation appears generally delayed at the first time point while the defect is clearly seen toward the 3′ end of the gene at later time points (Fig 6C). An interesting pattern of Pol II dynamics can be seen in

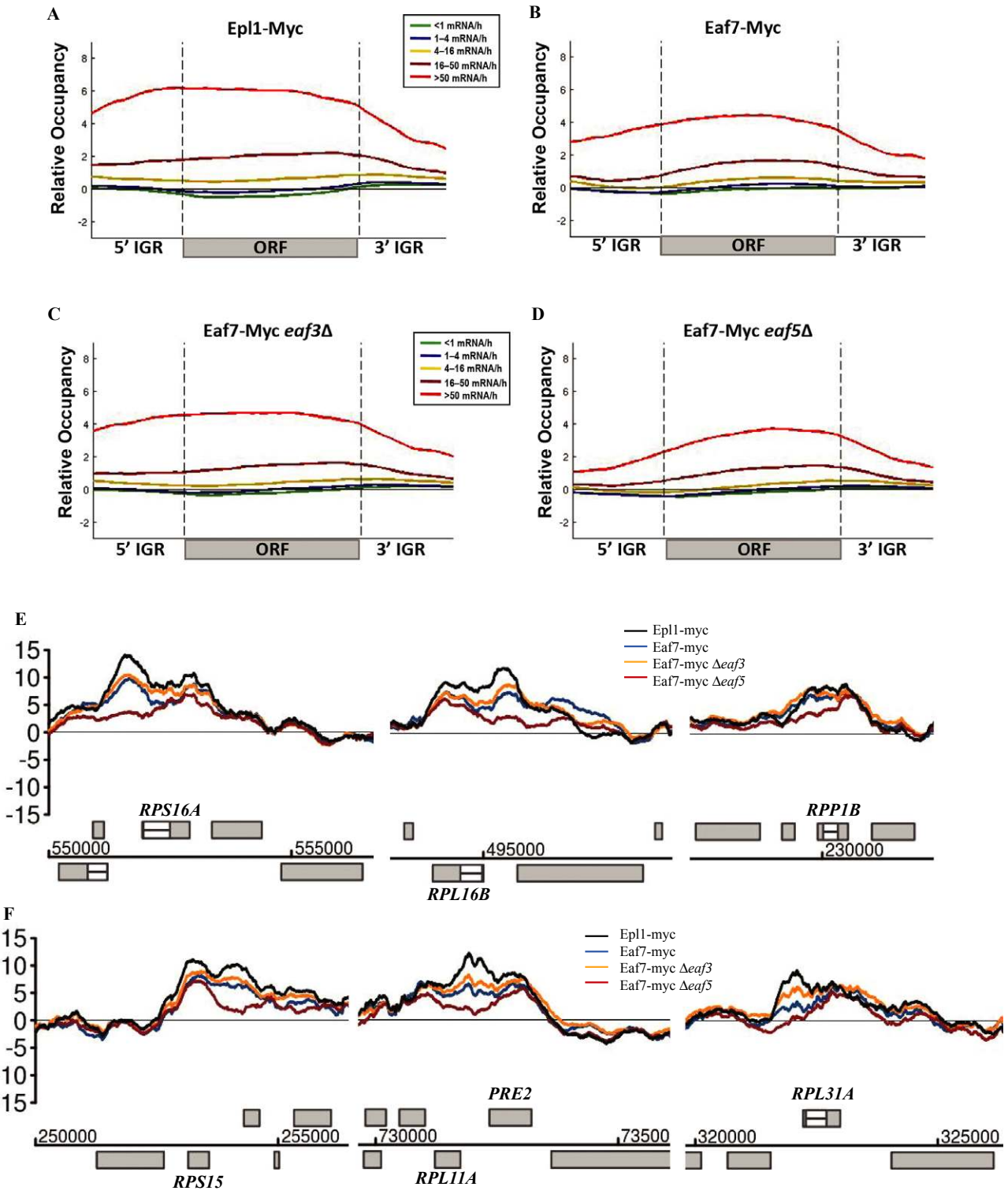

Figure 5. Eaf7 is globally associated to the coding regions of highly transcribed genes.

A–D Genome-wide average profiles of signals in relation to transcription activity obtained from high-resolution anti-Myc ChIP-chip from Epl1-Myc, Eaf7-Myc, Eaf7-Myc *eaf3*Δ, and Eaf7-Myc *eaf5*Δ strains. Similar to an approach by the Young lab (Pokholok *et al*, 2005), each ORF was divided into 40 bins (independent of gene length), and average enrichment values were calculated for each bin. Probes in promoter regions (500 bp upstream of coding start) and 3′UTR (500 bp downstream of coding stop) were assigned to 20 bins, respectively. Genes were divided into five classes according to their transcriptional frequency (Holstege *et al*, 1998), and the average enrichment value for each bin was plotted for all five transcriptional classes.

E, F Examples of signal profiles at six specific loci showing enrichment. Average signals are based on at least two independent experiments.

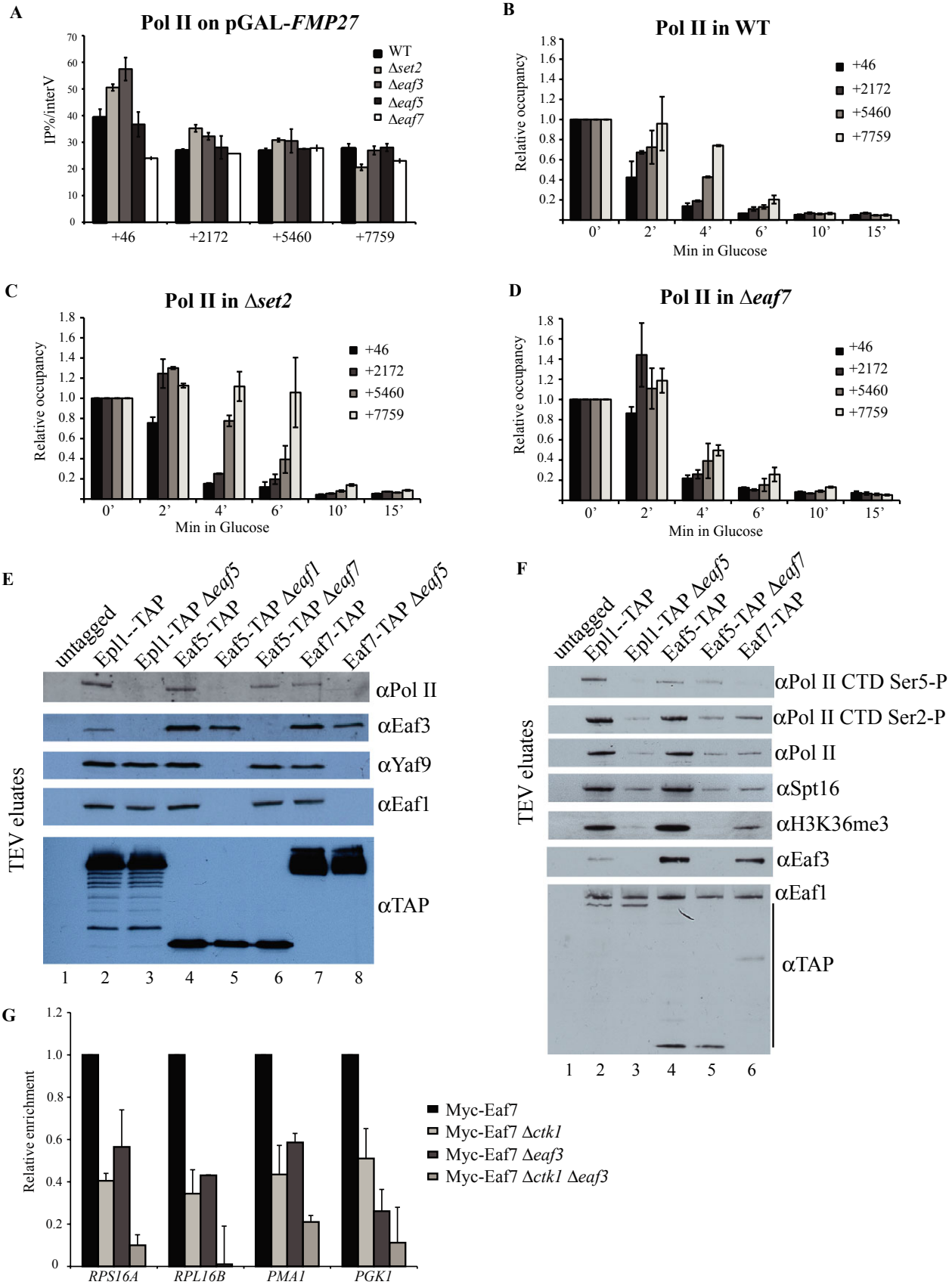

Figure 6. Eaf7 affects RNA Pol II processivity during transcription elongation and drives association with the isoform that carries the Ser2-P mark on its C-terminal domain.

A Steady-state levels of RNA pol II of the active pGAL-*FMP27* gene as measured by ChIP-qPCR.

B–D Time course of Pol II release during transcription repression of pGAL-*FMP27*. Cells were grown at 30°C in YP +2% galactose and glucose, which was added to a final concentration of 4% to repress genes under the control of the GAL promoter including *FMP27*. Cross-link was performed at 0, 2, 4, 6, 10, and 15 min after glucose addition, and the last wave of the RNA Pol II was followed using anti-Pol II (8WG16) antibody and primers corresponding to the indicated loci over *FMP27* coding region. Relative occupancy was calculated taking the ratio of the IP% at one locus versus the IP% at interV control locus at t = 2′, 4′, 6′, 10′, and 15′, divided by the same ratio at t = 0′, then considering that IP% at 0′ = 1. WT (B), *set2* (C) and *eaf7* (D) mutant strains were analyzed.

E Western blot analysis of TEV eluates from the indicated TAP-tagged fractions purified on IgG magnetic beads. Anti-TAP signals serve as loading controls and refer to Fig 2C to recall the effect of the different mutant backgrounds for the association of the trimer with the rest of NuA4.

F Western blot analysis similar to (E) but using antibodies specific for Ser5-P or Ser2-P isoforms of Pol II CTD, FACT subunit Spt16, and H3K36me3.

G Loss of Ctk1 kinase responsible for RNA Pol II CTD Ser2-P decreases Eaf7 association to coding regions, an effect exacerbated by concomitant loss of H3K36me-binding subunit Eaf3. ChIP-qPCR analysis of Eaf7-Myc association to the coding regions of *RPS16A* (+768), *RPL16B* (+784), *PMA1* (+104), and *PGK1* (+866) in the indicated mutant strains. IP/input signals were subtracted with the corresponding untagged signals and are shown relative to wild-type conditions.

Source data are available online for this figure.

the *eaf7* mutant where signals remain basically unchanged at all loci after 2 min of repression, followed 2 min later by a rapid disappearance throughout the coding region, most clearly at the 3′end of the gene (Fig 6D and Supplementary Fig S5). This result suggests a role of Eaf7 in Pol II processivity more than elongation rate, meaning that, in the mutant background, the polymerase tends to dissociate from the template (Mason & Struhl, 2005). In agreement with an important role during transcription elongation, the *eaf7* deletion mutant from the homozygous diploid yeast gene knockout collection was identified in a large-scale screen for mutants that show sensitivity to high concentration of 6AU and MPA (Riles *et al*, 2004).

NuA4 and Eaf5/7/3 interact with elongating RNA polymerase II

Based on the previous results and since it has been argued that both Rpd3S and NuA4 can interact with elongating RNA Pol II (Ginsburg *et al*, 2009; Drouin *et al*, 2010; Govind *et al*, 2010), we tested whether the Eaf5/7/3 trimer could also interact with RNAPII. We compared our Eaf7 genome-wide data with the signals previously obtained following the same protocol with the Rpb3 subunit of RNAPII (Schulze *et al*, 2011), and we observed high level of overlap between the signals throughout the transcription units (Supplementary Fig S6). Epl1, Eaf5, and Eaf7 were then used as TAP-tagged forms to investigate interaction with Pol II by Western blot on TEV eluates from IgG magnetic beads (Fig 6E). A clear Pol II signal is detected in all wild-type fractions but not in the untagged control. Using *eaf1* and *eaf5* mutant backgrounds that allow full separation of the trimer from the rest of NuA4, we find that NuA4 requires the Eaf5/7/3 trimer to bind RNAPII (Fig 6E, compare lanes 2 and 3). On the other hand, the presence of Eaf1/NuA4 enhances the association of Pol II with the trimer (lanes 4 and 5, 7 and 8). Interestingly, the loss of Eaf7 does not seem to affect the interaction (lanes 4 and 6). These data indicate that Eaf5 plays a critical role in NuA4-RNAPII interaction but also that other important points of contact might exist. Since *eaf5* and *eaf7* mutants show strong negative genetic interactions with genes encoding for Ctk1/3 (Mitchell *et al*, 2008; Wilmes *et al*, 2008; Bandyopadhyay *et al*, 2010), the main kinase responsible for phosphorylation of Pol II C-terminal domain on serine-2 of the repeats and the subsequent association of the Set2 methyltransferase (Xiao *et al*, 2003), we determined which isoform of phosphorylated elongating RNAPII associates with NuA4 and Eaf5/7/3. Interestingly, serine-5 phosphorylation by Kin28, which is associated with the early steps of elongation, is detected in both Epl1 and Eaf5 fractions, but not in Eaf7, and *EAF7* deletion does not affect interaction with Eaf5 (Fig 6F, lanes 2, 4, 5 and 6). In contrast, serine-2 phosphorylation, linked to the downstream elongating polymerase, is clearly detected in the Eaf7 fraction (lane 6). Importantly, while deletion of *EAF7* has no effect on RNAPII Ser5-P association with Eaf5, it has a clear detrimental effect on association of RNAPII Ser2-P (compare lanes 4 and 5). Altogether, these results argue that the Eaf5/7/3 associates with elongating polymerases and that Eaf7 favors interaction with the CTD Ser2-P isoform located further downstream in the coding regions of active genes, an interaction reminiscent of Set2 H3K36 methyltransferase and Rpd3S (Xiao *et al*, 2003; Drouin *et al*, 2010).

We can also detect signals for H3K36me3 in the TEV eluates, an interaction that clearly depends on the Eaf5/7/3 trimer, presumably through Eaf3 chromodomain (Fig. 6F). Thus, we postulate that a dual physical interaction is important over the coding region, one with the phosphorylated CTD of elongating polymerase and the other one with nucleosomes modified by the associated Set2 methyltransferase (similar to what is proposed for Rpd3S)(Drouin *et al*, 2010; Govind *et al*, 2010). To test this hypothesis, we performed ChIP-qPCR to analyze Eaf7 binding to coding regions in the absence of Ctk1, the main kinase for CTD Ser2. As shown in Fig. 6G, loss of Ctk1 clearly affects binding of Eaf7 to the body of several transcribed genes. Interestingly, the combined losses of Ctk1 and Eaf3 (interaction with H3K36me) cripple binding of Eaf7 to near background level.

The Eaf5/7/3 trimer plays a role in nucleosome destabilization during transcription elongation

Even with independent functions, the physical association of the Eaf5/7/3 trimer with NuA4 suggests a role in chromatin dynamics during transcription elongation. It has already been shown that NuA4 competes with Rpd3S *in vivo* (Biswas *et al*, 2008). Rpd3S is known to associate with elongating polymerase, which allows its binding to nucleosomes methylated on H3K36 by Set2 and their deacetylation (Carrozza *et al*, 2005; Joshi & Struhl, 2005; Keogh *et al*, 2005; Drouin *et al*, 2010; Govind *et al*, 2010). This action is thought to stabilize nucleosomes in the wake of elongating polymerases, preventing spurious transcription initiation (Carrozza *et al*, 2005; Li *et al*, 2007c). To investigate the role of NuA4 and Eaf5/7/3 in this pathway, we used a system designed by the Winston lab in

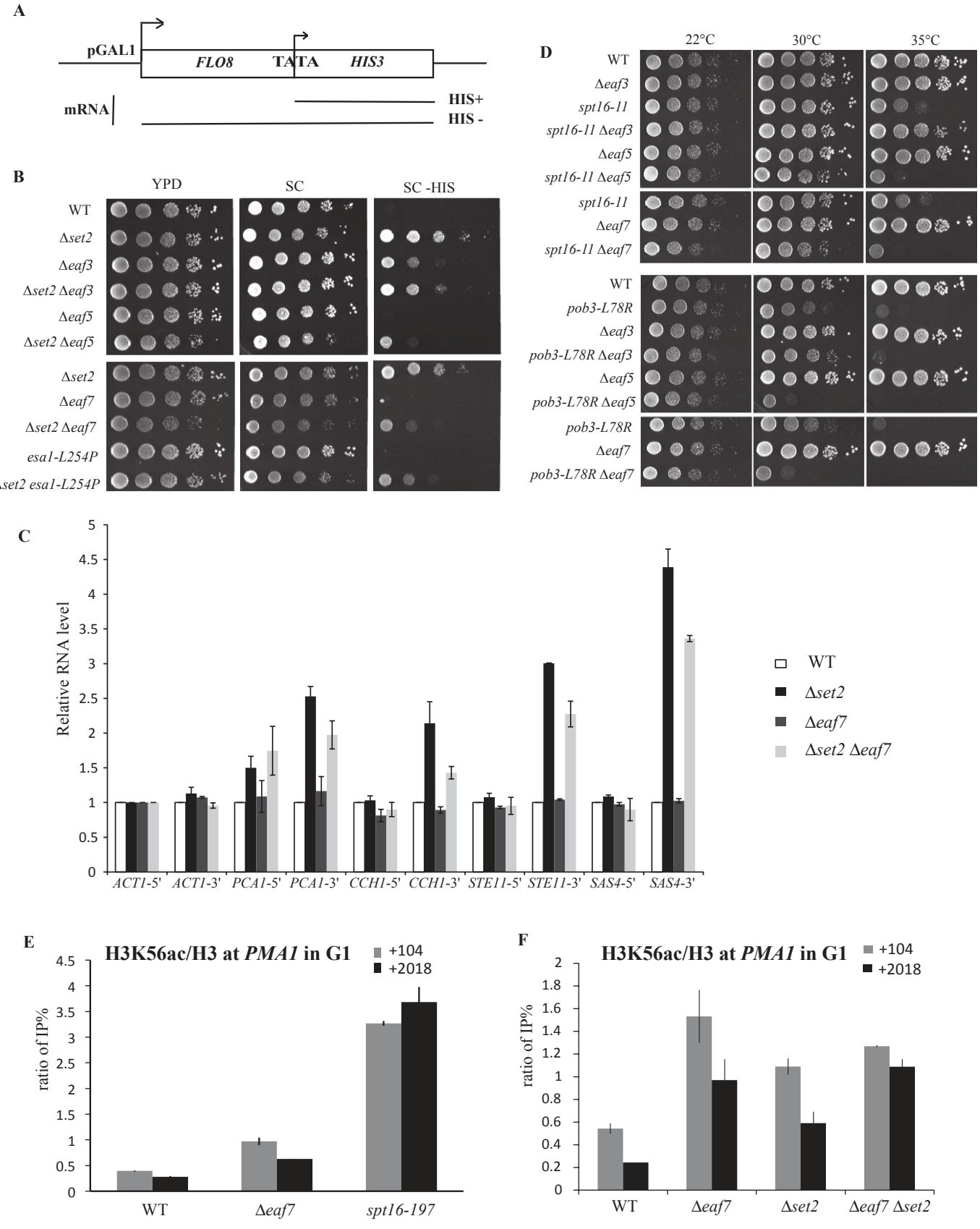

Figure 7. NuA4 and *eaf5/7/3* mutants partially suppress cryptic transcription induced by loss of Set2, and the trimer cooperates with FACT and H3K36me3 to block new histone incorporation on coding regions.

A Scheme of the *FLO8:HIS3* reporter construction. The *FLO8* gene is placed under the *GAL1* inducible promoter and is fused to the *HIS3* gene just after its internal TATA-like sequence (position +1,626bp). The HIS+ phenotype, through production of the small transcript of the HIS3 gene, reflects an internal/cryptic transcription initiation, whereas the HIS- phenotype is due to the normal transcription of the *FLO8* gene.

B *eaf3*, *eaf5*, and *eaf7* deletion mutants and *esa1-L254P* mutation affect cryptic transcription induced by loss of Set2. Serial tenfold dilutions of the indicated strains were spotted on YPD, SC, and SC-HIS plates. Cells were grown at 30°C for 3 days to detect the level of cryptic initiation within the *FLO8* gene.

C *eaf7* deletion mutant partially suppresses cryptic transcription induced by loss of Set2 on several genes *in vivo*. RT-qPCR was performed on total RNA isolated from the indicated strains with primers amplifying regions on the 5′ or 3′ end of genes in order to detect intragenic cryptic transcription initiation. Signals were corrected on ACT1 5′ control signal and shown relative to the wild-type strain. Error bars are based on four independent cultures.

D *EAF3*, *5*, *7* genetically interacts with the FACT chaperone subunits Spt16 and Pob3. Serial tenfold dilutions of indicated strains were spotted on YPD and grown at the indicated temperatures for 2–3 days. Deletion of *EAF5* and *EAF7* genes increases the thermosensitivity of the single *spt16-11* or *pob3-L78R* mutants, whereas deletion of *EAF3* gene suppresses *spt16-11* mutant sensitivity at 35°C.

E, F ChIP-qPCR analysis of histone exchange on the coding region of the transcriptionally active *PMA1* gene using the H3K56ac versus total H3 signal ratio after blocking the cells in G1 with alpha factor. A high ratio represents an elevated level of replication-independent new histone incorporation, which is significantly increased in the indicated mutant backgrounds (cells were also incubated for 1 h at 37°C in (E)).

which a *HIS3* reporter gene is integrated within the coding region of *FLO8*, next to a known cryptic TATA box that becomes active upon disruption of nucleosome maintenance during transcription elongation (Fig 7A)(Nourani *et al*, 2006; Cheung *et al*, 2008). In this system, deletion of *SET2* leads to cryptic initiation of *HIS3* transcription and growth in the absence of histidine in the media (Fig 7B). Deletion of *EAF3* also leads to growth in the absence of histidine because of its role in Rpd3S deacetylase activity, but to a somewhat lower level. In contrast, deletion of *EAF5* and *EAF7,* or mutation of Esa1 acetyltransferase subunit of NuA4 does not allow expression of *HIS3*. On the other hand, these same mutants do partially suppress *HIS3*-dependent growth of the *SET2* deletion. In these conditions, even *EAF3* deletion decreases growth of the *set2* mutant. To confirm these effects in the natural context and at the transcription level, we analyzed genes that were previously shown to produce intragenic cryptic transcripts in a *set2* mutant background (Venkatesh *et al*, 2012). Using reverse transcription-qPCR with primer sets corresponding to the 5′ end and the 3′end of these genes, we can clearly detect in *set2* mutant cells appearance of shorter transcripts that use cryptic initiation sites within the coding region (Fig 7C). Deletion of *EAF7* has no apparent effect on the expression of these genes but again partially suppresses the cryptic transcripts that arise in *set2* mutants. Altogether, these data indicate that NuA4 HAT activity and the Eaf5/7/3 trimer function contrary to the Set2-Rpd3S pathway, favoring nucleosome destabilization during the elongation process. Loss of this function partially suppresses the transcriptional defect caused by the loss of nucleosome methylation/deacetylation in the absence of Set2.

These results suggest that NuA4 and Eaf5/7/3 could help dissociate nucleosomes in front of the advancing polymerase before their Set2-stimulated reassembly and stabilization in its wake (Li *et al*, 2007a). In this model, histone chaperones such as Spt6 and FACT play a major role allowing transfer of histones from the front to the back of the polymerase (Avvakumov *et al*, 2011). Supporting the implication of the Eaf5/7/3 trimer in this process, we detect a physical interaction between Eaf7 and Spt16, a subunit of the FACT histone chaperone (Fig 6F). Furthermore, a negative genetic interaction is clearly detected between mutants in the FACT subunits (Spt16 and Pob3) and *eaf5*/*eaf7* mutants (Fig 7D). Such a role of Eaf5/7/3 in favoring nucleosome destabilization in front of the polymerase should lead to more stable nucleosomes in the mutant cells. Relative nucleosome stability can be more efficiently studied by measuring the dynamics of replication-independent exchange of histones at specific loci, as previously described (Rufiange *et al*, 2007). In this type of analysis, newly incorporated histones can be measured in cells blocked in G1 using the H3K56ac mark compared to total histone H3 signal in ChIP experiments. The values obtained at different loci reflect replication-independent histone exchange that occurs at these loci, which is higher at promoter regions and in the body of highly transcribed genes (Rufiange *et al*, 2007). In contrast to what we expected, we measure a significant increase of H3K56ac/H3 signal at *PMA1* in *eaf7* mutant cells, suggesting a higher level of histone exchange and less stable nucleosomes (Fig 7E). Similar results are obtained at other transcribed loci (Supplementary Fig S7A). It has been shown that higher incorporation of new histones can occur when old histones are not properly recycled from in front to behind the elongating polymerase. For example, this happens in cells defective for the FACT histone chaperone when H3-H4 redeposition is compromised, leading to increased incorporation of new histones (Jamai *et al*, 2009). Consistent with this concept, we obtain an even higher level of H3K56ac/H3 signal in *spt16* mutant cells (Fig. 7E). To determine whether augmented incorporation of new histones is linked to transcription, we compared signals at a non-transcribed control locus (Supplementary Fig S7B). In contrast to *spt16*, the *eaf7* mutant has a marginal effect on incorporation at the non-transcribed locus, suggesting after correction that the Eaf5/7/3 trimer and FACT have similar effect on the redeposition of histones evicted by elongating RNA polymerase (Supplementary Fig S7C). No further increase of new histone deposition is detected in *eaf7 spt16* double-mutant cells (Supplementary Fig S7D), and similar results are obtained with the inducible epitope-tagged H3 system to measure replication-independent new histone incorporation (Rufiange *et al*, 2007; data not shown).

It was recently reported that loss of Set2-mediated H3K36 methylation also leads to replication-independent increased incorporation of new histones at transcribed genes (Venkatesh *et al*, 2012). This is thought to occur through Rpd3S/deacetylation-mediated nucleosome stabilization, preventing the incorporation of new histones carrying the H3K56ac mark for *de novo* assembly (Smolle *et al*, 2013). We also detect increased incorporation of new histones in *set2* mutant cells, slightly lower than what is seen with the *eaf7* mutant, while the double-mutant cells showed a more even incorporation throughout the *PMA1* gene (Fig 7F). Altogether, these results implicate the Eaf7/5/3 trimer in nucleosome dynamics during transcription elongation, favoring RNA Pol II progression through associated nucleosome disruption and transfer for reassembly in its wake.

Discussion

In this study, we have analyzed poorly characterized subunits of the NuA4 histone acetyltransferase complex. We found that, while Eaf6 resides in the catalytic core of NuA4 (picNuA4), Eaf5 and Eaf7 are responsible for the association of the chromodomain protein Eaf3 to NuA4. Our biochemical data indicate that the Eaf5/7/3 subcomplex is not required for NuA4 structural integrity and is attached through an interaction between Eaf5 and Eaf1 (see Fig 2C). We also found that the Eaf5/7/3 trimer exists as a native complex outside of NuA4. We showed that *eaf5/7* mutant cells share similar phenotypes, in which some are shared with other components of NuA4 while others are specific to the trimer, supporting an independent function. Our work presents gene-specific localization data and high-resolution genome-wide mapping of NuA4 and Eaf5/7/3-binding sites. While both overlap greatly in their target genes and their correlation to transcriptional activity, they present different profiles over the transcription units. In comparison to previous lower resolution studies (Robert *et al*, 2004; Venters *et al*, 2011), NuA4 shows a high level of binding throughout the coding regions of these highly transcribed genes, with a polarity of higher enrichment toward the transcription start site and promoter region (Fig 5A). In contrast, Eaf7 shows a polarity of higher enrichment toward the middle of the coding region (Fig 5B). This difference in profiles is exacerbated when the analysis is done in an *eaf5* mutant strain, which disrupts any possible interaction between Eaf7 and NuA4 (Fig 5D–F, Supplementary Fig S3A). Surprisingly, while loss of Eaf5 specifically depletes Eaf7 from promoter regions without greatly affecting coding regions, loss of Eaf3 and its H3K36me-binding chromodomain does not prevent Eaf7 from binding to the body of the gene (Fig 5C, E–F; Supplementary Fig S3A). This clearly demonstrates that Eaf7 requires NuA4 to be bound to the promoter but neither NuA4 nor Eaf3-H3K36me for its association with the body of active genes. We present data supporting an additional mechanism favoring binding to transcribed regions, related to what has been suggested for the Eaf3-containing Rpd3S complex (Drouin *et al*, 2010; Govind *et al*, 2010). While elongating RNA polymerase II physically interacts with the NuA4 complex (confirming previous findings; Ginsburg *et al*, 2009) and the Eaf5/7/3 trimer, loss of Eaf7 specifically depletes the Pol II isoform that is phosphorylated on the serine-2 of its C-terminal domain repeats (Fig. 6F). Importantly, loss of the CTD Ser2 kinase, Ctk1, decreases binding of Eaf7 to coding regions (Fig 6G). Loss of both Ctk1 and Eaf3 cripples Eaf7 binding to near background levels, indicating that RNAPII CTD Ser2-P and nucleosomes bearing H3K36me2/3 form a dual interaction surface for the trimer on the body of transcribed genes, at a distance from the transcription start site.

In trying to decipher the precise function of the Eaf5/7/3, we accumulated data supporting a role in nucleosome dynamics during transcription elongation, favoring destabilization in front of the polymerase, but also stabilizing nucleosomes in its wake along with the Set2-H3K36me-Rpd3S pathway (see Fig 8). This model is

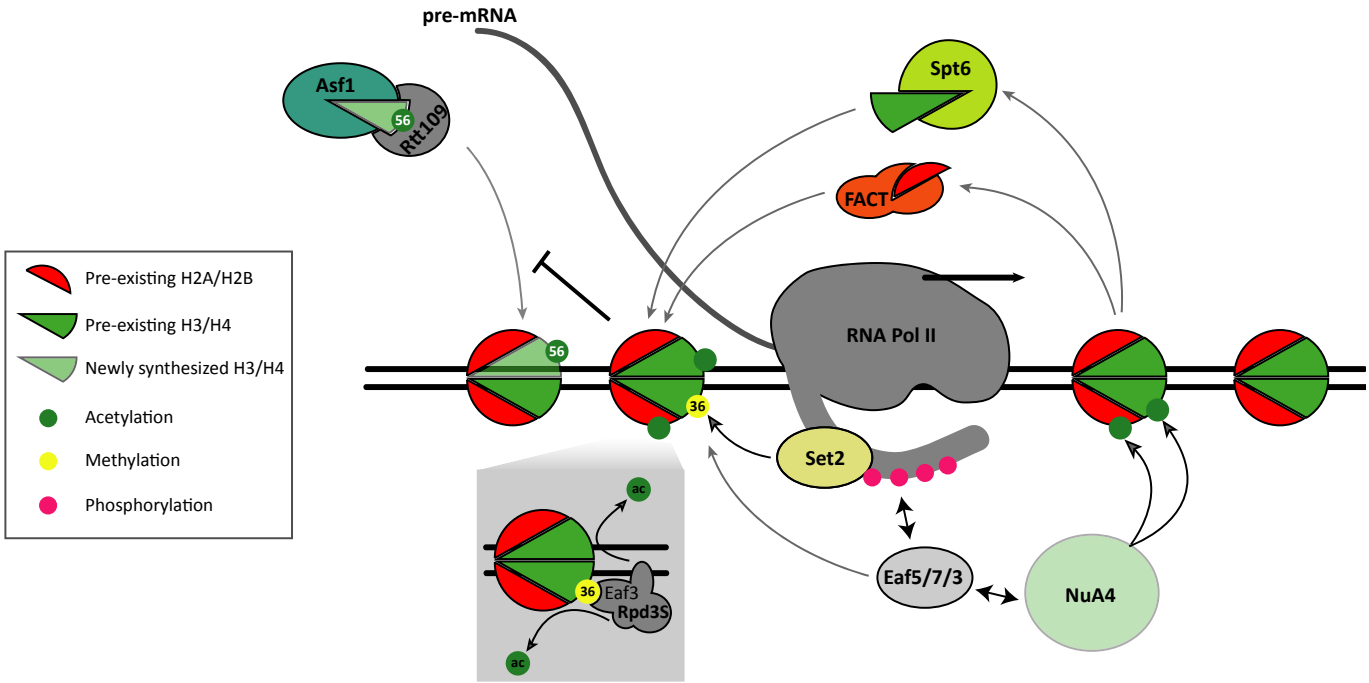

Figure 8. Model for the roles of the Eaf5/7/3 trimer in nucleosome dynamics during transcription elongation.
Physical interactions of the Eaf5/7/3 are shown, including association with the NuA4 HAT complex, binding to RNA pol II CTD phosphorylated on serine 2, and interaction with H3K36me3-containing nucleosome through Eaf3 chromodomain. Set2 histone methyltransferase also binds P-Ser2 CTD leading to H3K36 methylation. The trimer-containing NuA4 is thought to acetylate nucleosomes in front of the polymerase, leading to their disruption in cooperation with FACT and Spt6 histone chaperones. H3K36me3-binding Eaf3 is also a subunit of the Rpd3S HDAC complex, leading to deacetylation of reassembled nucleosomes behind the polymerase. These recycled nucleosomes are thought to suppress histone exchange/new histone incorporation (H3K56ac) and cryptic transcription initiation. Thus, the Eaf5/7/3 trimer follows the elongating polymerase to help nucleosome disruption in front and reassembly in its wake.

supported by a decrease in elongation processivity of Pol II and partial suppression of spurious transcription appearing in *set2* mutant cells, as well as an increase in replication-independent histone exchange in *eaf7* mutant cells. One could easily envision the Eaf5/7/3 trimer traveling with Pol II CTD phosphorylated on Ser2, leading to interaction with H3K36me-containing nucleosomes through the Eaf3 chromodomain. Destabilization of nucleosomes in front of the polymerase would function in part through tethering of NuA4 acetyltransferase activity. Stabilization of the nucleosomes behind the polymerase, blocking histone exchange/incorporation of new histones, would function through cooperation with histone chaperones to recycle the disrupted nucleosomes (Fig. 8). Supporting this model, we can detect physical interaction between the Eaf5/7/3 trimer and the FACT histone chaperone in cellular extracts (Fig 6F).

Questions remain about other possible functions of the Eaf5/7/3 trimer. Consistent with the striking structural conservation of NuA4 from yeast to human, the Eaf7 homolog in higher eukaryotes was found associated with the human Tip60 complex (Cai *et al*, 2003). In this report, it was apparent that the homologous protein, called MRGBP, was interacting directly with MRG15, the human homolog of Eaf3. Gel filtration and a large-scale proteomic study also indicate that the MRGBP-MRG15 complex exists independently of the Tip60 complex (Kirkwood *et al*, 2013). Results in our lab (K. Jacquet and J. Côté; in preparation) as well as recent published work (Gowher *et al*, 2012) also demonstrate the independent function of MRGBP-MRG15. Interestingly, methylation of H3K36 at exon–intron junctions plays a role in co-transcriptional mRNA splicing, and MRG15 was shown to regulate alternative splicing (reviewed in Luco *et al*, 2011). Furthermore, the MRGBP-MRG15 dimer has now been linked to this process in relation to peaks of elongating polymerases carrying Ser2-P on their C-terminal domain (Gowher *et al*, 2012). Since Eaf5 is the only NuA4 subunit having no homolog in human cells, these strong analogies suggest that the MRGBP-MRG15 dimer is the functional homolog of the yeast Eaf5/7/3 trimer. Keeping this in mind, it is striking to note that most of the intron-containing genes in the yeast genome are in fact highly transcribed, encoding for ribosomal proteins (RP) and bound by NuA4 and Eaf7. We could not detect significant defect of the mRNA splicing process using a reporter plasmid (Teem & Rosbash, 1983) in *eaf5/7* mutant cells (data not shown). Definitive answers about a possible role of the Eaf5/7/3 trimer in mRNA splicing will require additional work in more physiological conditions. It is possible that a role in RNA processing is linked to the strong genetic interaction detected with the SWR1 complex (Supplementary Fig S2A) (Krogan *et al*, 2004). SWR1-C and its bromodomain-containing subunit Bdf1 have been recently linked to transcription elongation and identified as important regulators of mRNA splicing (Santisteban *et al*, 2011; Albulescu *et al*, 2012).

Interestingly, secondary mass spectrometry hits in Eaf7-TAP purifications included proteins associated with the nuclear exosome (Dis3, Srp1, Kap95; Synowsky *et al*, 2009; data not shown). Furthermore, *eaf5* and *eaf7* mutants show negative genetic interactions with several components of the nuclear exosome and the THO-TREX mRNA export machinery (Wilmes *et al*, 2008). We can detect a reproducible small increase of transcription read-through in *eaf5/7* mutants using a reporter plasmid (Carroll *et al*, 2004), suggesting some defect in exosome activity/3′ end formation (data not shown). While these results require additional investigation in more physiological systems, they suggest that the Eaf5/7/3 trimer could indeed play a role in co-transcriptional RNA processing and maturation.

Altogether, the results presented in this study identified an exciting new functional module in the NuA4 histone acetyltransferase, as well as an independent trimeric complex. An important role during transcription elongation is attributed to the trimer, in part through tethering of NuA4 activity, but also independently. This NuA4-independent role of the Eaf5/7/3 trimer forces us to reexamine several large-scale genetic studies (e.g., SGA/E-MAP) that used solely *eaf5* and *eaf7* interactions as measurement of NuA4 function. The Eaf5/7/3 trimer is an atypical transcription elongation factor as it not only functions in nucleosome disruption to allow better RNAPII processivity, but also facilitates nucleosome recycling/stability behind the polymerase, suppressing histone exchange. It will be most interesting to extend our analysis, dissecting the precise mechanisms by which the Eaf5/7/3 trimer affects both nucleosome disruption in front of the polymerase and refolding in its wake. This will also help to determine additional roles and functional conservation with human MRGBP-MRG15 in regulating mRNA splicing/processing.

Materials and Methods

Yeast strains, plasmids and growth assays

All the strain genotypes used in this study are based on the S288c background (LPY3431; Clarke *et al*, 1999 or BY4741(Resgen)) and are listed in Supplementary Table S1. PCR-based integrations were used to make deletion strains, and epitope-tagging with KanMX, HisMX, and NatR (plasmid p4339) selection cassettes followed standard protocols (Longtine *et al*, 1998; Tong *et al*, 2001). Plasmid pHPL32URA was constructed as follows: *EAF5* was amplified from yeast genomic DNA and cloned with BamHI and SmaI in pFEMXE (described in Boudreault *et al*, 2003) to give pF32L. *EAF5* promoter was also amplified from genomic DNA and cloned with HindIII and NcoI in pF32L to give pHPL32. BglII inserts containing *URA3* from pFL38 and *LEU2* from pHPL32 were swapped to give pHPL32Ura. Plasmid pHPL32ORFEaf7URA was constructed by swapping *EAF5* by *EAF7* in the pHPL32Ura plasmid using BamHI and PvuII. pSet2-FlagURA was a generous gift from B. Strahl. Deletion mutants were introduced in strains carrying pGAL-*FMP27*, pGAL-*FLO8-HIS3*, and pGAL-Flag-H3/Myc-H3 described in Rufiange *et al* (2007) and Cheung *et al* (2008). The double deletion strains were generated by the plasmid shuffle technique where the first deletion is covered by the same gene on a *URA3* plasmid followed by the second gene deletion. Yeast strains were then grown overnight in SC at 30°C, diluted to an OD_{600} of 0.25, and grown for 3 h in SC. 10-fold serial dilutions of cultures were spotted onto SC or SC supplemented with 0.1% 5′ FOA to evict the *URA3* containing plasmid. For the yeast spot sensitivity assay, yeast strains were grown overnight at 30°C in YPD, diluted to an OD_{600} of 0.5, and grown for 3 h in YPD. Then 10-fold serial dilutions of cultures were spotted onto different media and grown at the indicated temperatures. YPD plates containing drugs such as methyl methanesulfonate (MMS; 0.015%), rapamycin (25 nM), 6-AzaUracil (6AU; 200 μg/ml), mycophenolic acid (MPA; 100 μg/ml), formamide (3%), and caffeine (6 mM) were used to test for resistance compared to YPD control plates.

Purification of protein complexes

TAP purification was performed as initially reported by Seraphin and colleagues (Puig *et al*, 2001) with modifications described in Auger *et al* (2008). Purified fractions were assayed for HAT activity and by Western blot as described (Allard *et al*, 1999), and specific protein bands were excised from gels and identified by tandem mass spectrometry at the CHUL proteomic platform. When indicated, calmodulin or TEV elutions were further fractionated by gel filtration on a Superose 6 column as described (Altaf *et al*, 2010). For co-IP experiments, TEV elutions were obtained using magnetic beads (Dynal) on which IgG were manually pre-bound, as described (Mitchell *et al*, 2008). Antibodies for NuA4 subunits used in Western blot analysis have been described ((Auger *et al*, 2008) and references therein), while anti-CTD Ser5-P and Ser2-P were obtained from Millipore (3E8, 310), anti-total RNA pol II from Covance (8WG16), anti-H3K36me3 from Abcam (ab9050), and anti-Spt16 was a gift from Tim Formosa.

Reverse-transcription-qPCR

Total RNA was purified by hot phenol extraction from 10 ml of cells grown to an OD_{600} of 0.6 to 1.0. 5 μg of RNA was treated with the Turbo DNase kit (Ambion), and 2 μg of DNA-free RNA was synthesized into cDNA using qScript cDNA supermix (Quanta Biosciences) according to the manufacturer's instructions. cDNA was then diluted and quantified by real-time qPCR (Syber Green, Roche) on the LC480 LightCycler (Roche) using primers near the 5′ and 3′ end of the gene (sequences available upon request). Relative amounts were normalized to *ACT1* 5′. All values are expressed relative to the wild-type value, set at 1, and error bars denote standard deviations of a biological quadruplicate (four independent cultures, two distinct experiments).

Chromatin Immunoprecipitation (ChIPs)

ChIP experiments were essentially performed as previously described (Utley *et al*, 2005). Briefly, cell culture of 200 ml of appropriate media grown at 0.5–1 OD_{600} was cross-linked for 20 min with 1% formaldehyde. For the replication-independent histone exchange assays, cells were blocked in G1 with alpha factor as described (Rufiange *et al*, 2007). After cross-link, the reaction was stopped by adding glycine at a final concentration of 200 mM. Cell lysate was obtained by bead beating cells with glass beads in FA lysis buffer (50 mM HEPES pH 7.5, 140 mM NaCl, 1 mM EDTA pH 8, 1% Triton, 0.1% Na deoxycholate) to reach 70–80% of cells disrupted. Chromatin was sheared by sonication (Bioruptor) to 200–500 bp fragments. Immunoprecipitations were performed on 100 μg of chromatin with 2 μl of anti-Myc, 2 μl of anti-Pol II (8WG16), 0.3 μl of anti-H3K56ac (Upstate, 07-677), and 0.5 μg of anti-H3 (Abcam, ab1791) antibodies for at least 12 h at 4°C. ChIPs were then incubated with protein A or G sepharose matrix (GE Healthcare) for 5hrs at 4°C or with Dynabeads coated with protein G (Invitrogen) for the Myc-tagged proteins. After washes with 140 mM NaCl FA Lysis Buffer, 500 mM NaCl FA Lysis Buffer, Wash Buffer #2 (10 mM Tris pH8, 250 mM LiCl, 0.5% NP40, 0.5% Na deoxycholate, 1 mM EDTA), and TE, the immunoprecipitated chromatin was eluted from the beads with elution buffer (50 mM Tris, 10 mM EDTA, 1% SDS) for 15 min at 65°C and reverse cross-linked for 12 h at the same temperature. ChIPs were treated 15 min with RNase A and proteinase K, and DNA was purified by standard phenol-chloroform extraction and precipitated. DNA was then quantified by real-time qPCR (Syber Green, Roche) on the LC480 LightCycler (Roche). All ChIPs were performed in at least two independent experiments, and data presented in figures represent the average between the biological replicates with the corresponding standard errors. A large non-coding region of chromosome V (positions 9716–9863) was used as control locus (Nourani *et al*, 2004). All primer sequences are available upon request.

ChIP-on-chip and data analysis

ChIP-on-chip experiments were performed as described previously (Schulze *et al*, 2009) with minor modifications. In brief, yeast cells (500 ml) were grown in a rich medium to an OD_{600} of 0.5–0.6 and were cross-linked with 1% formaldehyde for 60 min before chromatin was extracted. The chromatin was sonicated (Bioruptor, Diagenode; Sparta, NJ: 15 cycles, 30 s on/off, high setting) to yield an average DNA fragment of 500 bp. Anti-Myc (5 μl, Sigma) antibodies were coupled to 60 μl of protein A magnetic beads (Invitrogen). After reversal of the cross-linking and DNA purification, the immunoprecipitated and input DNA was amplified to about 6 μg aRNA using T7 RNA polymerase in two rounds. Samples were labeled with biotin, and the immunoprecipitated and input samples were hybridized to Affymetrix 1.0R S. cerevisiae microarrays, which are comprised of over 3.2 million probes covering the complete genome. Probes (25-mer) are tiled at an average of 5 bp resolution, creating an overlap of approximately 20 bp between adjacent probes.

Data analysis was performed as described previously (Schulze *et al*, 2009) and was submitted to the ArrayExpress database under accession number E-MTAB-1780. Annotations for ORFs, ARSs, and centromeres were derived from the SGD database. An ORF was termed enriched if at least 50% of all probes had a MAT score above a threshold of 1.5. Promoters were defined as enriched if all probes 300 bp upstream of the transcriptional start site were above the MAT score cutoff. Promoters that overlap with ORFs of other genes were not considered. Given the transient nature of NuA4 subunits binding to chromatin, we determined a high confidence data set intersecting the two replicates after quantile normalization and performed subsequent analysis with the normalized data. A list of all transcription start and end sites for 4,868 transcripts was kindly provided by Harm van Bakel (Timothy Hughes' lab). The CHROMATRA graphs were generated as described previously (Hentrich *et al*, 2012). Enrichment scores of each Myc-tagged protein were calculated across nucleosome-sized intervals of 150 bp and color-coded for all known 4,868 transcripts, which were aligned according to their transcription start sites (TSS) and sorted by their length or by length as well as transcriptional frequency (Holstege *et al*, 1998).

Supplementary information for this article is available online: http://emboj.embopress.org

Acknowledgements

We are grateful to Anne Rufiange, Dominique Cronier, and Nathalie Bouchard for experiments performed at different stages of this work. We are indebted to Rhea Utley for the construction of some strains used in this study and critical

reading of the manuscript, and John Yates for original mass spec analysis that allowed identification of Eaf7 in NuA4. We also wish to thank David Stillman, Swami Venkatesh, Bing Li, Jerry Workman, Andréanne Auger, François Robert, and Rhea Utley for stimulating discussions. We thank John Lucchesi, Patrick Grant, David Stillman, Song Tan, Tim Formosa, and Brian Strahl for anti-Eaf3, anti-Tra1, anti-Arp4/anti-Sin3, anti-Yng2, anti-Spt16, and p*SET2*/URA3, respectively, and David Stillman for strains used during this study. This work was supported by grants from the Canadian Institutes of Health Research (CIHR) to A.N. (MOP-81245), M.S.K. (MOP-119383), and J.C. (MOP-14308). M.S.K is a Senior Fellow of the Canadian Institute for Advanced Research. A.N. and J.C. hold Canada Research Chairs.

Author contributions

DR, MC, AW, A-LS, NL, JS, VC, JM-S, and SP performed experiments. DR, MC, AW, A-LS, NL, JS, AN, MSK, and JC designed experiments and interpreted the results. JC wrote the manuscript.

Conflict of interest

The authors declare that they have no conflict of interest.

References

Albulescu LO, Sabet N, Gudipati M, Stepankiw N, Bergman ZJ, Huffaker TC, Pleiss JA (2012) A quantitative, high-throughput reverse genetic screen reveals novel connections between Pre-mRNA splicing and 5' and 3' end transcript determinants. *PLoS Genet* 8: e1002530

Allard S, Utley RT, Savard J, Clarke A, Grant P, Brandl CJ, Pillus L, Workman JL, Cote J (1999) NuA4, an essential transcription adaptor/histone H4 acetyltransferase complex containing Esa1p and the ATM-related cofactor Tra1p. *EMBO J* 18: 5108–5119

Altaf M, Auger A, Covic M, Cote J (2009) Connection between histone H2A variants and chromatin remodeling complexes. *Biochem Cell Biol* 87: 35–50

Altaf M, Auger A, Monnet-Saksouk J, Brodeur J, Piquet S, Cramet M, Bouchard N, Lacoste N, Utley RT, Gaudreau L, Cote J (2010) NuA4-dependent acetylation of nucleosomal histones H4 and H2A directly stimulates incorporation of H2A.Z by the SWR1 complex. *J Biol Chem* 285: 15966–15977

Auger A, Galarneau L, Altaf M, Nourani A, Doyon Y, Utley RT, Cronier D, Allard S, Cote J (2008) Eaf1 is the platform for NuA4 molecular assembly that evolutionarily links chromatin acetylation to ATP-dependent exchange of histone H2A variants. *Mol Cell Biol* 28: 2257–2270

Avvakumov N, Nourani A, Cote J (2011) Histone chaperones: modulators of chromatin marks. *Mol Cell* 41: 502–514

Avvakumov N, Lalonde ME, Saksouk N, Paquet E, Glass KC, Landry AJ, Doyon Y, Cayrou C, Robitaille GA, Richard DE, Yang XJ, Kutateladze TG, Cote J (2012) Conserved molecular interactions within the HBO1 acetyltransferase complexes regulate cell proliferation. *Mol Cell Biol* 32: 689–703

Babiarz JE, Halley JE, Rine J (2006) Telomeric heterochromatin boundaries require NuA4-dependent acetylation of histone variant H2A.Z in Saccharomyces cerevisiae. *Genes Dev* 20: 700–710

Bandyopadhyay S, Mehta M, Kuo D, Sung MK, Chuang R, Jaehnig EJ, Bodenmiller B, Licon K, Copeland W, Shales M, Fiedler D, Dutkowski J, Guenole A, van Attikum H, Shokat KM, Kolodner RD, Huh WK, Aebersold R, Keogh MC, Krogan NJ *et al* (2010) Rewiring of genetic networks in response to DNA damage. *Science* 330: 1385–1389

Bannister AJ, Kouzarides T (2011) Regulation of chromatin by histone modifications. *Cell Res* 21: 381–395

Bird AW, Yu DY, Pray-Grant MG, Qiu Q, Harmon KE, Megee PC, Grant PA, Smith MM, Christman MF (2002) Acetylation of histone H4 by Esa1 is required for DNA double-strand break repair. *Nature* 419: 411–415

Biswas D, Takahata S, Stillman DJ (2008) Different genetic functions for the Rpd3(L) and Rpd3(S) complexes suggest competition between NuA4 and Rpd3(S). *Mol Cell Biol* 28: 4445–4458

Boudreault AA, Cronier D, Selleck W, Lacoste N, Utley RT, Allard S, Savard J, Lane WS, Tan S, Cote J (2003) Yeast enhancer of polycomb defines global Esa1-dependent acetylation of chromatin. *Genes Dev* 17: 1415–1428

Brown CE, Howe L, Sousa K, Alley SC, Carrozza MJ, Tan S, Workman JL (2001) Recruitment of HAT complexes by direct activator interactions with the ATM-related Tra1 subunit. *Science* 292: 2333–2337

Cai Y, Jin J, Tomomori-Sato C, Sato S, Sorokina I, Parmely TJ, Conaway RC, Conaway JW (2003) Identification of new subunits of the multiprotein mammalian TRRAP/TIP60-containing histone acetyltransferase complex. *J Biol Chem* 278: 42733–42736

Carey M, Li B, Workman JL (2006) RSC exploits histone acetylation to abrogate the nucleosomal block to RNA polymerase II elongation. *Mol Cell* 24: 481–487

Carroll KL, Pradhan DA, Granek JA, Clarke ND, Corden JL (2004) Identification of cis elements directing termination of yeast nonpolyadenylated snoRNA transcripts. *Mol Cell Biol* 24: 6241–6252

Carrozza MJ, Li B, Florens L, Suganuma T, Swanson SK, Lee KK, Shia WJ, Anderson S, Yates J, Washburn MP, Workman JL (2005) Histone H3 methylation by Set2 directs deacetylation of coding regions by Rpd3S to suppress spurious intragenic transcription. *Cell* 123: 581–592

Cheung V, Chua G, Batada NN, Landry CR, Michnick SW, Hughes TR, Winston F (2008) Chromatin- and transcription-related factors repress transcription from within coding regions throughout the Saccharomyces cerevisiae genome. *PLoS Biol* 6: e277

Choy JS, Kron SJ (2002) NuA4 subunit Yng2 function in intra-S-phase DNA damage response. *Mol Cell Biol* 22: 8215–8225

Clarke AS, Lowell JE, Jacobson SJ, Pillus L (1999) Esa1p is an essential histone acetyltransferase required for cell cycle progression. *Mol Cell Biol* 19: 2515–2526

Downs JA, Allard S, Jobin-Robitaille O, Javaheri A, Auger A, Bouchard N, Kron SJ, Jackson SP, Cote J (2004) Binding of chromatin-modifying activities to phosphorylated histone H2A at DNA damage sites. *Mol Cell* 16: 979–990

Doyon Y, Cote J (2004) The highly conserved and multifunctional NuA4 HAT complex. *Curr Opin Genet Dev* 14: 147–154

Doyon Y, Selleck W, Lane WS, Tan S, Cote J (2004) Structural and functional conservation of the NuA4 histone acetyltransferase complex from yeast to humans. *Mol Cell Biol* 24: 1884–1896

Doyon Y, Cayrou C, Ullah M, Landry AJ, Cote V, Selleck W, Lane WS, Tan S, Yang XJ, Cote J (2006) ING tumor suppressor proteins are critical regulators of chromatin acetylation required for genome expression and perpetuation. *Mol Cell* 21: 51–64

Drouin S, Laramee L, Jacques PE, Forest A, Bergeron M, Robert F (2010) DSIF and RNA polymerase II CTD phosphorylation coordinate the recruitment of Rpd3S to actively transcribed genes. *PLoS Genet* 6: e1001173

Durant M, Pugh BF (2007) NuA4-directed chromatin transactions throughout the Saccharomyces cerevisiae genome. *Mol Cell Biol* 27: 5327–5335

Eisen A, Utley RT, Nourani A, Allard S, Schmidt P, Lane WS, Lucchesi JC, Cote J (2001) The yeast NuA4 and Drosophila MSL complexes contain

homologous subunits important for transcription regulation. *J Biol Chem* 276: 3484 – 3491

Friis RM, Wu BP, Reinke SN, Hockman DJ, Sykes BD, Schultz MC (2009) A glycolytic burst drives glucose induction of global histone acetylation by picNuA4 and SAGA. *Nucleic Acids Res* 37: 3969 – 3980

Galarneau L, Nourani A, Boudreault AA, Zhang Y, Heliot L, Allard S, Savard J, Lane WS, Stillman DJ, Cote J (2000) Multiple links between the NuA4 histone acetyltransferase complex and epigenetic control of transcription. *Mol Cell* 5: 927 – 937

Ginsburg DS, Govind CK, Hinnebusch AG (2009) NuA4 lysine acetyltransferase Esa1 is targeted to coding regions and stimulates transcription elongation with Gcn5. *Mol Cell Biol* 29: 6473 – 6487

Govind CK, Qiu H, Ginsburg DS, Ruan C, Hofmeyer K, Hu C, Swaminathan V, Workman JL, Li B, Hinnebusch AG (2010) Phosphorylated Pol II CTD recruits multiple HDACs, including Rpd3C(S), for methylation-dependent deacetylation of ORF nucleosomes. *Mol Cell* 39: 234 – 246

Gowher H, Brick K, Camerini-Otero RD, Felsenfeld G (2012) Vezf1 protein binding sites genome-wide are associated with pausing of elongating RNA polymerase II. *Proc Natl Acad Sci USA* 109: 2370 – 2375

Hentrich T, Schulze JM, Emberly E, Kobor MS (2012) CHROMATRA: a Galaxy tool for visualizing genome-wide chromatin signatures. *Bioinformatics* 28: 717 – 718

Holstege FC, Jennings EG, Wyrick JJ, Lee TI, Hengartner CJ, Green MR, Golub TR, Lander ES, Young RA (1998) Dissecting the regulatory circuitry of a eukaryotic genome. *Cell* 95: 717 – 728

Jamai A, Puglisi A, Strubin M (2009) Histone chaperone spt16 promotes redeposition of the original h3-h4 histones evicted by elongating RNA polymerase. *Mol Cell* 35: 377 – 383

Joo YJ, Kim JH, Kang UB, Yu MH, Kim J (2011) Gcn4p-mediated transcriptional repression of ribosomal protein genes under amino-acid starvation. *EMBO J* 30: 859 – 872

Joshi AA, Struhl K (2005) Eaf3 chromodomain interaction with methylated H3-K36 links histone deacetylation to Pol II elongation. *Mol Cell* 20: 971 – 978

Keogh MC, Kurdistani SK, Morris SA, Ahn SH, Podolny V, Collins SR, Schuldiner M, Chin K, Punna T, Thompson NJ, Boone C, Emili A, Weissman JS, Hughes TR, Strahl BD, Grunstein M, Greenblatt JF, Buratowski S, Krogan NJ (2005) Cotranscriptional set2 methylation of histone H3 lysine 36 recruits a repressive Rpd3 complex. *Cell* 123: 593 – 605

Keogh MC, Mennella TA, Sawa C, Berthelet S, Krogan NJ, Wolek A, Podolny V, Carpenter LR, Greenblatt JF, Baetz K, Buratowski S (2006) The Saccharomyces cerevisiae histone H2A variant Htz1 is acetylated by NuA4. *Genes Dev* 20: 660 – 665

Kim HS, Vanoosthuyse V, Fillingham J, Roguev A, Watt S, Kislinger T, Treyer A, Carpenter LR, Bennett CS, Emili A, Greenblatt JF, Hardwick KG, Krogan NJ, Bahler J, Keogh MC (2009) An acetylated form of histone H2A.Z regulates chromosome architecture in Schizosaccharomyces pombe. *Nat Struct Mol Biol* 16: 1286 – 1293

Kirkwood KJ, Ahmad Y, Larance M, Lamond AI (2013) Characterization of Native Protein Complexes and Protein Isoform Variation Using Size-fractionation-based Quantitative Proteomics. *Mol Cell Proteomics* 12: 3851 – 3873

Kobor MS, Venkatasubrahmanyam S, Meneghini MD, Gin JW, Jennings JL, Link AJ, Madhani HD, Rine J (2004) A protein complex containing the conserved Swi2/Snf2-related ATPase Swr1p deposits histone variant H2A.Z into euchromatin. *PLoS Biol* 2: E131

Krogan NJ, Keogh MC, Datta N, Sawa C, Ryan OW, Ding H, Haw RA, Pootoolal J, Tong A, Canadien V, Richards DP, Wu X, Emili A, Hughes TR, Buratowski S, Greenblatt JF (2003) A Snf2 family ATPase complex required for recruitment of the histone H2A variant Htz1. *Mol Cell* 12: 1565 – 1576

Krogan NJ, Baetz K, Keogh MC, Datta N, Sawa C, Kwok TC, Thompson NJ, Davey MG, Pootoolal J, Hughes TR, Emili A, Buratowski S, Hieter P, Greenblatt JF (2004) Regulation of chromosome stability by the histone H2A variant Htz1, the Swr1 chromatin remodeling complex, and the histone acetyltransferase NuA4. *Proc Natl Acad Sci USA* 101: 13513 – 13518

Le Masson I, Yu DY, Jensen K, Chevalier A, Courbeyrette R, Boulard Y, Smith MM, Mann C (2003) Yaf9, a novel NuA4 histone acetyltransferase subunit, is required for the cellular response to spindle stress in yeast. *Mol Cell Biol* 23: 6086 – 6102

Li B, Carey M, Workman JL (2007a) The role of chromatin during transcription. *Cell* 128: 707 – 719

Li B, Gogol M, Carey M, Lee D, Seidel C, Workman JL (2007b) Combined action of PHD and chromo domains directs the Rpd3S HDAC to transcribed chromatin. *Science* 316: 1050 – 1054

Li B, Gogol M, Carey M, Pattenden SG, Seidel C, Workman JL (2007c) Infrequently transcribed long genes depend on the Set2/Rpd3S pathway for accurate transcription. *Genes Dev* 21: 1422 – 1430

Lin YY, Qi Y, Lu JY, Pan X, Yuan DS, Zhao Y, Bader JS, Boeke JD (2008) A comprehensive synthetic genetic interaction network governing yeast histone acetylation and deacetylation. *Genes Dev* 22: 2062 – 2074

Lin YY, Lu JY, Zhang J, Walter W, Dang W, Wan J, Tao SC, Qian J, Zhao Y, Boeke JD, Berger SL, Zhu H (2009) Protein acetylation microarray reveals that NuA4 controls key metabolic target regulating gluconeogenesis. *Cell* 136: 1073 – 1084

Longtine MS, McKenzie A 3rd, Demarini DJ, Shah NG, Wach A, Brachat A, Philippsen P, Pringle JR (1998) Additional modules for versatile and economical PCR-based gene deletion and modification in Saccharomyces cerevisiae. *Yeast* 14: 953 – 961

Lu JY, Lin YY, Sheu JC, Wu JT, Lee FJ, Chen Y, Lin MI, Chiang FT, Tai TY, Berger SL, Zhao Y, Tsai KS, Zhu H, Chuang LM, Boeke JD (2011) Acetylation of yeast AMPK controls intrinsic aging independently of caloric restriction. *Cell* 146: 969 – 979

Luco RF, Allo M, Schor IE, Kornblihtt AR, Misteli T (2011) Epigenetics in alternative pre-mRNA splicing. *Cell* 144: 16 – 26

Marston AL, Tham WH, Shah H, Amon A (2004) A genome-wide screen identifies genes required for centromeric cohesion. *Science* 303: 1367 – 1370

Mason PB, Struhl K (2005) Distinction and relationship between elongation rate and processivity of RNA polymerase II in vivo. *Mol Cell* 17: 831 – 840

Millar CB, Xu F, Zhang K, Grunstein M (2006) Acetylation of H2AZ Lys 14 is associated with genome-wide gene activity in yeast. *Genes Dev* 20: 711 – 722

Mitchell L, Lambert JP, Gerdes M, Al-Madhoun AS, Skerjanc IS, Figeys D, Baetz K (2008) Functional dissection of the NuA4 histone acetyltransferase reveals its role as a genetic hub and that Eaf1 is essential for complex integrity. *Mol Cell Biol* 28: 2244 – 2256

Mitchell L, Lau A, Lambert JP, Zhou H, Fong Y, Couture JF, Figeys D, Baetz K (2011) Regulation of septin dynamics by the Saccharomyces cerevisiae lysine acetyltransferase NuA4. *PLoS ONE* 6: e25336

Mizuguchi G, Shen X, Landry J, Wu WH, Sen S, Wu C (2004) ATP-driven exchange of histone H2AZ variant catalyzed by SWR1 chromatin remodeling complex. *Science* 303: 343 – 348

Morillon A, Karabetsou N, Nair A, Mellor J (2005) Dynamic lysine methylation on histone H3 defines the regulatory phase of gene transcription. *Mol Cell* 18: 723 – 734

Musselman CA, Lalonde ME, Cote J, Kutateladze TG (2012) Perceiving the epigenetic landscape through histone readers. *Nat Struct Mol Biol* 19: 1218 – 1227

Nourani A, Doyon Y, Utley RT, Allard S, Lane WS, Cote J (2001) Role of an ING1 growth regulator in transcriptional activation and targeted histone acetylation by the NuA4 complex. *Mol Cell Biol* 21: 7629 – 7640

Nourani A, Utley RT, Allard S, Cote J (2004) Recruitment of the NuA4 complex poises the PHO5 promoter for chromatin remodeling and activation. *EMBO J* 23: 2597 – 2607

Nourani A, Robert F, Winston F (2006) Evidence that Spt2/Sin1, an HMG-like factor, plays roles in transcription elongation, chromatin structure, and genome stability in Saccharomyces cerevisiae. *Mol Cell Biol* 26: 1496 – 1509

Pokholok DK, Harbison CT, Levine S, Cole M, Hannett NM, Lee TI, Bell GW, Walker K, Rolfe PA, Herbolsheimer E, Zeitlinger J, Lewitter F, Gifford DK, Young RA (2005) Genome-wide map of nucleosome acetylation and methylation in yeast. *Cell* 122: 517 – 527

Puig O, Caspary F, Rigaut G, Rutz B, Bouveret E, Bragado-Nilsson E, Wilm M, Seraphin B (2001) The tandem affinity purification (TAP) method: a general procedure of protein complex purification. *Methods* 24: 218 – 229

Reid JL, Iyer VR, Brown PO, Struhl K (2000) Coordinate regulation of yeast ribosomal protein genes is associated with targeted recruitment of Esa1 histone acetylase. *Mol Cell* 6: 1297 – 1307

Reid JL, Moqtaderi Z, Struhl K (2004) Eaf3 regulates the global pattern of histone acetylation in Saccharomyces cerevisiae. *Mol Cell Biol* 24: 757 – 764

Reines D (2003) Use of RNA yeast polymerase II mutants in studying transcription elongation. *Methods Enzymol* 371: 284 – 292

Riles L, Shaw RJ, Johnston M, Reines D (2004) Large-scale screening of yeast mutants for sensitivity to the IMP dehydrogenase inhibitor 6-azauracil. *Yeast* 21: 241 – 248

Robert F, Pokholok DK, Hannett NM, Rinaldi NJ, Chandy M, Rolfe A, Workman JL, Gifford DK, Young RA (2004) Global position and recruitment of HATs and HDACs in the yeast genome. *Mol Cell* 16: 199 – 209

Rohde JR, Cardenas ME (2003) The tor pathway regulates gene expression by linking nutrient sensing to histone acetylation. *Mol Cell Biol* 23: 629 – 635

Rufiange A, Jacques PE, Bhat W, Robert F, Nourani A (2007) Genome-wide replication-independent histone H3 exchange occurs predominantly at promoters and implicates H3 K56 acetylation and Asf1. *Mol Cell* 27: 393 – 405

Santisteban MS, Hang M, Smith MM (2011) Histone variant H2A.Z and RNA polymerase II transcription elongation. *Mol Cell Biol* 31: 1848 – 1860

Schulze JM, Jackson J, Nakanishi S, Gardner JM, Hentrich T, Haug J, Johnston M, Jaspersen SL, Kobor MS, Shilatifard A (2009) Linking cell cycle to histone modifications: SBF and H2B monoubiquitination machinery and cell-cycle regulation of H3K79 dimethylation. *Mol Cell* 35: 626 – 641

Schulze JM, Hentrich T, Nakanishi S, Gupta A, Emberly E, Shilatifard A, Kobor MS (2011) Splitting the task: Ubp8 and Ubp10 deubiquitinate different cellular pools of H2BK123. *Genes Dev* 25: 2242 – 2247

Shen X, Mizuguchi G, Hamiche A, Wu C (2000) A chromatin remodelling complex involved in transcription and DNA processing. *Nature* 406: 541 – 544

Shilatifard A (2006) Chromatin modifications by methylation and ubiquitination: implications in the regulation of gene expression. *Annu Rev Biochem* 75: 243 – 269

Smith ER, Eisen A, Gu W, Sattah M, Pannuti A, Zhou J, Cook RG, Lucchesi JC, Allis CD (1998) ESA1 is a histone acetyltransferase that is essential for growth in yeast. *Proc Natl Acad Sci USA* 95: 3561 – 3565

Smolle M, Workman JL, Venkatesh S (2013) reSETting chromatin during transcription elongation. *Epigenetics* 8: 10 – 15.

Suganuma T, Workman JL (2011) Signals and combinatorial functions of histone modifications. *Annu Rev Biochem* 80: 473 – 499

Sun B, Hong J, Zhang P, Dong X, Shen X, Lin D, Ding J (2008) Molecular basis of the interaction of Saccharomyces cerevisiae Eaf3 chromo domain with methylated H3K36. *J Biol Chem* 283: 36504 – 36512

Synowsky SA, van Wijk M, Raijmakers R, Heck AJ (2009) Comparative multiplexed mass spectrometric analyses of endogenously expressed yeast nuclear and cytoplasmic exosomes. *J Mol Biol* 385: 1300 – 1313

Teem JL, Rosbash M (1983) Expression of a beta-galactosidase gene containing the ribosomal protein 51 intron is sensitive to the rna2 mutation of yeast. *Proc Natl Acad Sci USA* 80: 4403 – 4407

Tong AH, Evangelista M, Parsons AB, Xu H, Bader GD, Page N, Robinson M, Raghibizadeh S, Hogue CW, Bussey H, Andrews B, Tyers M, Boone C (2001) Systematic genetic analysis with ordered arrays of yeast deletion mutants. *Science* 294: 2364 – 2368

Uprety B, Lahudkar S, Malik S, Bhaumik SR (2012) The 19S proteasome subcomplex promotes the targeting of NuA4 HAT to the promoters of ribosomal protein genes to facilitate the recruitment of TFIID for transcriptional initiation in vivo. *Nucleic Acids Res* 40: 1969 – 1983

Utley RT, Ikeda K, Grant PA, Cote J, Steger DJ, Eberharter A, John S, Workman JL (1998) Transcriptional activators direct histone acetyltransferase complexes to nucleosomes. *Nature* 394: 498 – 502

Utley RT, Lacoste N, Jobin-Robitaille O, Allard S, Cote J (2005) Regulation of NuA4 histone acetyltransferase activity in transcription and DNA repair by phosphorylation of histone H4. *Mol Cell Biol* 25: 8179 – 8190

Venkatesh S, Smolle M, Li H, Gogol MM, Saint M, Kumar S, Natarajan K, Workman JL (2012) Set2 methylation of histone H3 lysine 36 suppresses histone exchange on transcribed genes. *Nature* 489: 452 – 455

Venters BJ, Wachi S, Mavrich TN, Andersen BE, Jena P, Sinnamon AJ, Jain P, Rolleri NS, Jiang C, Hemeryck-Walsh C, Pugh BF (2011) A comprehensive genomic binding map of gene and chromatin regulatory proteins in Saccharomyces. *Mol Cell* 41: 480 – 492

Wilmes GM, Bergkessel M, Bandyopadhyay S, Shales M, Braberg H, Cagney G, Collins SR, Whitworth GB, Kress TL, Weissman JS, Ideker T, Guthrie C, Krogan NJ (2008) A genetic interaction map of RNA-processing factors reveals links between Sem1/Dss1-containing complexes and mRNA export and splicing. *Mol Cell* 32: 735 – 746

Xiao T, Hall H, Kizer KO, Shibata Y, Hall MC, Borchers CH, Strahl BD (2003) Phosphorylation of RNA polymerase II CTD regulates H3 methylation in yeast. *Genes Dev* 17: 654 – 663

Xu C, Cui G, Botuyan MV, Mer G (2008) Structural basis for the recognition of methylated histone H3K36 by the Eaf3 subunit of histone deacetylase complex Rpd3S. *Structure* 16: 1740 – 1750

Yi C, Ma M, Ran L, Zheng J, Tong J, Zhu J, Ma C, Sun Y, Zhang S, Feng W, Zhu L, Le Y, Gong X, Yan X, Hong B, Jiang FJ, Xie Z, Miao D, Deng H, Yu L (2012) Function and molecular mechanism of acetylation in autophagy regulation. *Science* 336: 474 – 477

Yun M, Wu J, Workman JL, Li B (2011) Readers of histone modifications. *Cell Res* 21: 564 – 578

Zentner GE, Henikoff S (2013) Regulation of nucleosome dynamics by histone modifications. *Nat Struct Mol Biol* 20: 259 – 266

Zhang H, Richardson DO, Roberts DN, Utley R, Erdjument-Bromage H, Tempst P, Cote J, Cairns BR (2004) The Yaf9 component of the SWR1 and NuA4 complexes is required for proper gene expression, histone H4 acetylation, and Htz1 replacement near telomeres. *Mol Cell Biol* 24: 9424 – 9436

Zhou BO, Wang SS, Xu LX, Meng FL, Xuan YJ, Duan YM, Wang JY, Hu H, Dong X, Ding J, Zhou JQ (2010) SWR1 complex poises heterochromatin boundaries for antisilencing activity propagation. *Mol Cell Biol* 30: 2391 – 2400